





ORIGINAL RESEARCH

SWAP70 Overexpression Protects Against Pathological Cardiac Hypertrophy in a TAK1-Dependent Manner

Qiaofeng Qian , MD;* Fengjiao Hu, MD;* Wenjun Yu, MD;* Dewen Leng, MD; Yang Li, MD; Hongjie Shi, MD; Dawei Deng , MM; Kehan Ding, MM; Chuan Liang , MD; Jinping Liu , MD

BACKGROUND: Pathological cardiac hypertrophy is regarded as a critical precursor and independent risk factor of heart failure, and its inhibition prevents the progression of heart failure. Switch-associated protein 70 (SWAP70) is confirmed important in immunoregulation, cell maturation, and cell transformation. However, its role in pathological cardiac hypertrophy remains unclear.

METHODS AND RESULTS: The effects of SWAP70 on pathological cardiac hypertrophy were investigated in *Swap70* knockout mice and *Swap70* overexpression/knockdown cardiomyocytes. Bioinformatic analysis combined with multiple molecular biological methodologies were adopted to elucidate the mechanisms underlying the effects of SWAP70 on pathological cardiac hypertrophy. Results showed that SWAP70 protein levels were significantly increased in failing human heart tissues, experimental transverse aortic constriction–induced mouse hypertrophic hearts, and phenylephrine-stimulated isolated primary cardiomyocytes. Intriguingly, phenylephrine treatment decreased the lysosomal degradation of SWAP70 by disrupting the interaction of SWAP70 with granulin precursor. In vitro and in vivo experiments revealed that *Swap70* knockdown/knockout accelerated the progression of pathological cardiac hypertrophy, while *Swap70* overexpression restrained the cardiomyocyte hypertrophy. SWAP70 restrained the binding of transforming growth factor β -activated kinase 1 (TAK1) and TAK1 binding protein 1, thus blocking the phosphorylation of TAK1 and downstream c-Jun N-terminal kinase/P38 signaling. TAK1 interacted with the N-terminals (1–192) of SWAP70. *Swap70* (193–585) overexpression failed to inhibit cardiac hypertrophy when the TAK1–SWAP70 interaction was disrupted. Either inhibiting the phosphorylation or suppressing the expression of TAK1 rescued the exaggerated cardiac hypertrophy induced by *Swap70* knockdown.

CONCLUSIONS: SWAP70 suppressed the progression of cardiac hypertrophy, possibly by inhibiting the mitogen-activated protein kinases signaling pathway in a TAK1-dependent manner, and lysosomes are involved in the regulation of SWAP70 expression level.

Key Words: cardiac hypertrophy ■ granulin precursor ■ heart failure ■ mitogen-activated protein kinases ■ SWAP70

The adult mammalian heart contains \approx 65% to 80% by volume and 30% to 40% by number of cardiomyocytes.¹ The size of the heart and cardiomyocyte after birth is closely related to the size or metabolic requirements of the human body. Diseases such as hypertension, coronary heart disease, and valvular disorders

can lead to cardiomyocyte enlargement and further pathological cardiac hypertrophy, which is regarded as an adaptive myocardial response to pressure overload.² Constant stress damage to the heart eventually leads to myocardial systolic dysfunction, cytoskeleton remodeling, fibrosis, chamber dilation, increased risk of

Correspondence to: Jinping Liu, MD, PhD, Chuan Liang, MD, PhD, Department of Cardiovascular Surgery, Zhongnan Hospital of Wuhan University, 169 Donghu Road, Wuhan 430071, China. Email: liujinping@znhospital.cn, wuhanliangchuan@hotmail.com

*Q. Qian, F. Hu, and W. Yu contributed equally.

Supplemental Material is available at <https://www.ahajournals.org/doi/suppl/10.1161/JAHA.122.028628>

For Sources of Funding and Disclosures, see page 16.

© 2023 The Authors. Published on behalf of the American Heart Association, Inc., by Wiley. This is an open access article under the terms of the [Creative Commons Attribution-NonCommercial-NoDerivs](https://creativecommons.org/licenses/by-nc-nd/4.0/) License, which permits use and distribution in any medium, provided the original work is properly cited, the use is non-commercial and no modifications or adaptations are made.

JAHA is available at: www.ahajournals.org/journal/jaha

CLINICAL PERSPECTIVE

What Is New?

- Generation of *Swap70* knockout mice and *Swap70* overexpression/knockdown primary cardiomyocytes revealed the protective effect of switch-associated protein 70 (SWAP70) on myocardial hypertrophy.
- Granulin precursor regulates the protein degradation of SWAP70 through lysosomes and reduces the degradation of SWAP70 by reducing the binding to SWAP70 under hypertrophic stimuli. SWAP70 inhibits cardiomyocyte hypertrophy by inhibiting transforming growth factor β -activated kinase 1–transforming growth factor β -activated kinase 1 binding protein 1 interaction, thus inhibiting the activation of the downstream transforming growth factor β -activated kinase 1–JNK-P38 pathway.

What Are the Clinical Implications?

- Our results indicated that SWAP70 may be a potential target for preventing cardiac hypertrophy, and the study on the upstream and downstream regulation of SWAP70 may provide ideas for future clinical studies.

Nonstandard Abbreviations and Acronyms

GRN	granulin precursor
JNK	c-Jun N-terminal kinase
MAPK	mitogen-activated protein kinase
MYH7/β-MHC	β -myosin-heavy-chain
NRVMs	neonatal rat ventricular myocytes
SWAP70	switch-associated protein 70
TAB1	transforming growth factor β -activated kinase 1 binding protein 1
TAC	transverse aortic constriction
TAK1	transforming growth factor β -activated kinase 1
WT	wild-type

circulatory failure, and even death.^{3,4} Pathological cardiac hypertrophy is a critical precursor and independent risk factor for heart failure.^{5,6} Evidence indicates that inhibition of pathological cardiac hypertrophy can effectively prevent heart failure.⁷ Through the exploration of related pathways and their corresponding mechanisms, great progress has been achieved in the control of hypertension and treatment of secondary cardiac hypertrophy

attributable to other diseases. On the other hand, mechanisms, including cell metabolism, immune response, translational regulation, and posttranscriptional control neglected previously, have been demonstrated to negatively or positively regulate the progression of pathological cardiac hypertrophy.^{7–9} Further studies about the corresponding cellular signaling pathways, such as phosphoinositide 3-kinase or mitogen-activated protein kinase (MAPK) pathways, explored their unique roles in the various forms of hypertrophy.^{10–12} Today, although increasingly advanced medical treatments can improve the symptoms of heart failure, they cannot stop the progression of the disease or reverse the pathological progression.^{13,14} Exploration on the underlying mechanisms of pathological myocardial hypertrophy is essential to delay or even reverse the progression of cardiac hypertrophy.

Switch-associated protein 70 (SWAP70) is a rho guanine nucleotide exchange factor belonging to a small family of only 2 members, SWAP70 and FDCP 6 homolog (DEF6), which are originally discovered in B and T cells, respectively.¹⁵ SWAP70, which has a unique protein structure and functional characteristics, plays important roles in normal cellular processes, including immunoregulation, cellular morphological changes, and cell maturation.^{16–18} Although research on SWAP70 is mainly focused on immune cells (B cells, dendritic cells, and mast cells), studies on other non-immune cells, such as liver cells,¹⁹ fibroblasts,²⁰ blood cells,²¹ and osteoclasts,²² have also revealed a unique role of SWAP70 in disease progression. Deletion of *Swap70* can lead to limited immune protection,^{23–25} decreased cell invasion,^{16,26} and reduced cell differentiation and maturation.^{18,27} For example, *Swap70* deficiency can lead to poor B cell migration.²⁵ *Swap70* knockout mouse embryo fibroblasts (MEFs) grow more slowly and express less invasive phenotypes than wild-type MEFs.²⁶ *Swap70* deficiency in mice causes the accumulation of hematopoietic stem and precursor cells and reduces the differentiation of hematopoietic stem cells.²⁷

The viability and functional status of cardiomyocytes, as terminally differentiated cells, are critical to maintaining normal heart function. The MAPK pathway, which we find can be regulated by SWAP70 and inhibits the progression of nonalcoholic steatohepatitis,¹⁹ appears closely related to pathological cardiac hypertrophy and plays a key role in its progression.^{10,28} Hyperactivation of the MAPK pathway can aggravate pathological cardiac hypertrophy, whereas inhibition of this pathway causes opposite results.^{29,30} However, the relationship between SWAP70 and pathological hypertrophy remains to be established.

The present study aimed to examine the role of SWAP70 in pathological cardiac hypertrophy, with a focus on the MAPK pathway. The mechanisms

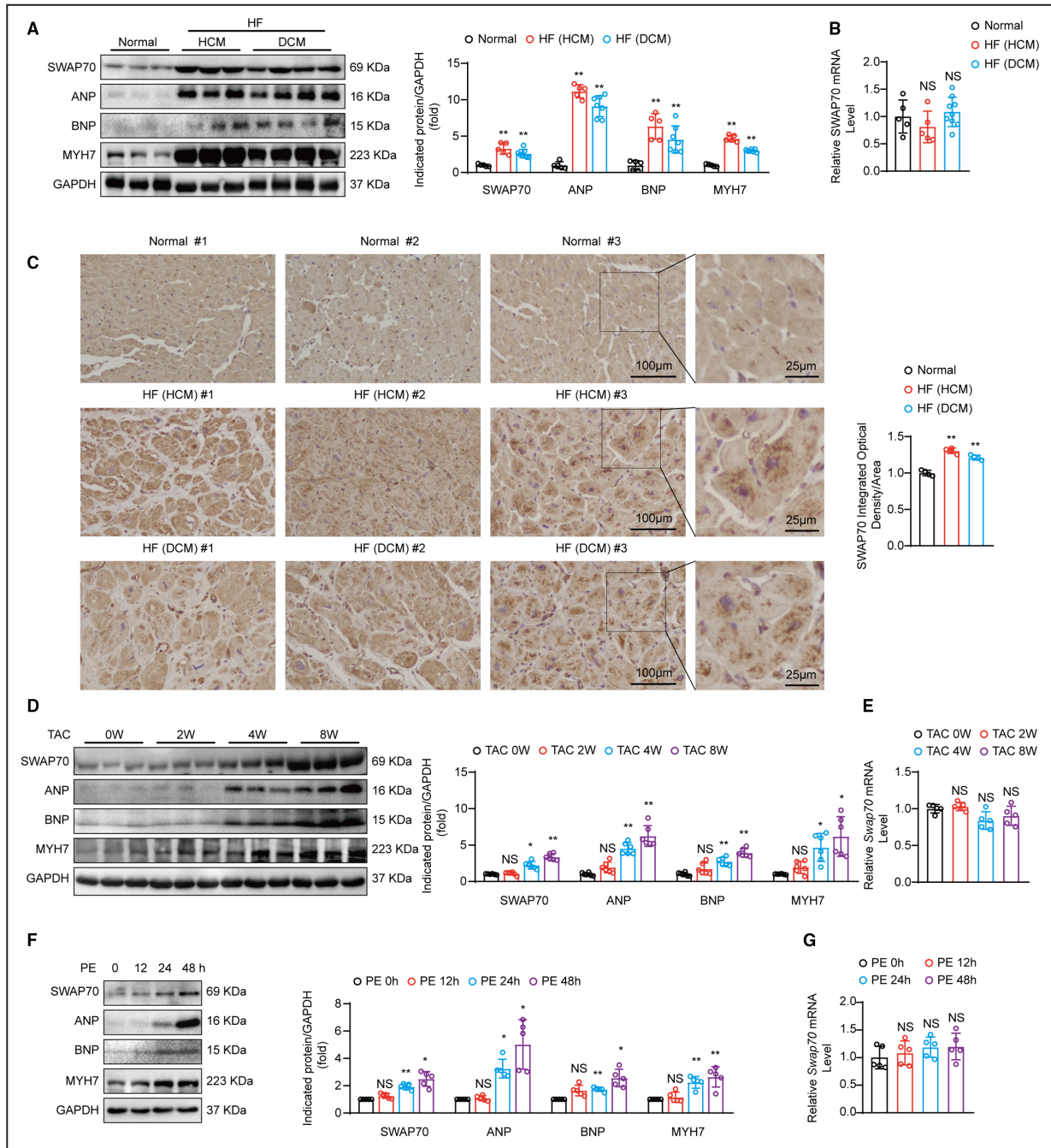


Figure 1. SWAP70 protein level is increased in response to hypertrophic stimuli.

A, Immunoblotting and quantitation of SWAP70, ANP, BNP, MYH7/ β -MHC protein levels in human heart tissues from normal donors (n=5), HCM heart failure patients (n=5), and DCM heart failure patients (n=7). **B**, Relative mRNA levels of SWAP70 in human heart tissues from normal donors (n=5), HCM heart failure patients (n=5), and DCM heart failure patients (n=9) (NS: left, $P=0.90$; right, $P=1.00$). **C**, Left, expression of SWAP70 in human tissues from normal donors or heart failure patients arise from HCM or DCM. Right, quantitation results of immunohistochemical staining (n=4). **D**, Protein levels and quantitation results of SWAP70, ANP, BNP, MYH7 in mice hearts subjected to TAC surgery at the indicated time points (n=6). **E**, Relative mRNA levels of *Swap70* in mice heart tissues after TAC operation at indicated time points (n=5) (NS: left, $P=1.00$; middle, $P=0.11$; right, $P=0.81$). **F**, Protein levels and quantitation results of SWAP70, ANP, BNP, MYH7 in NRVMs with ph PE (50 μ mol/L) treatment at indicated time points (n=5 independent experiments). **G**, Relative mRNA levels of *Swap70* in NRVMs with PE (50 μ mol/L) treatment at indicated time points (n=5 independent experiments) (NS: left, $P=1.00$; middle, $P=1.00$; right, $P=0.93$). Data are shown as mean \pm SD. One-way ANOVA with Bonferroni's post hoc analysis (**A** through **C**, **E**, **G**, MYH7 in **F**) or with Tamhane T2 post hoc test (MYH7 in **A**, **D**, **F**) was used. * $P<0.05$; ** $P<0.01$ for indicated group vs control group. NS (no significance for indicated group vs control group. ANP indicates atrial natriuretic peptide; BNP, B-type natriuretic peptide; DCM, dilated cardiomyopathy; HCM, hypertrophic cardiomyopathy; MYH7/ β -MHC, β -myosin-heavy-chain; NRVMs, neonatal rat ventricular myocytes; NS, no significance; PE, phenylephrine; SWAP70, switch-associated protein 70; and TAC, transverse aortic constriction.

underlying the regulation of SWAP70 protein expression were also investigated. This study may serve as a foundation for developing a strategy to prevent the progression of pathological cardiac hypertrophy.

METHODS

The data that support the findings of this study are available from the corresponding author upon reasonable request. See Data S1 and Tables S1 through S3 for detailed methods and materials used in the establishment of mouse models, detection of corresponding indicators, generation of *Swap70* knockout mice, isolation of primary neonatal rat ventricular myocytes (NRVMs) and cell culture, histological staining, immunofluorescence staining, plasmid construction and adenovirus infection, immunoblot analysis, quantitative real-time polymerase chain reaction, immunoprecipitation assay, and RNA sequencing.

Human Heart Samples

Left ventricular tissue specimens were procured from patients with end-stage heart failure undergoing heart transplantation for hypertrophic cardiomyopathy or dilated cardiomyopathy, and normal left ventricular tissue specimens were collected from heart donors identified unsuitable for transplantation for noncardiac reasons. All heart tissue specimens were stored in liquid nitrogen or soaked in 4% paraformaldehyde. All

human samples were obtained with written informed consent from the patients or their families and after authorization by the Hospital Committee for Investigation in Humans. All human sample collections were approved by the Human Research Ethics Committee of Zhongnan Hospital of Wuhan University (2022075K) and consistent with the principles outlined in the Declaration of Helsinki.

Mice

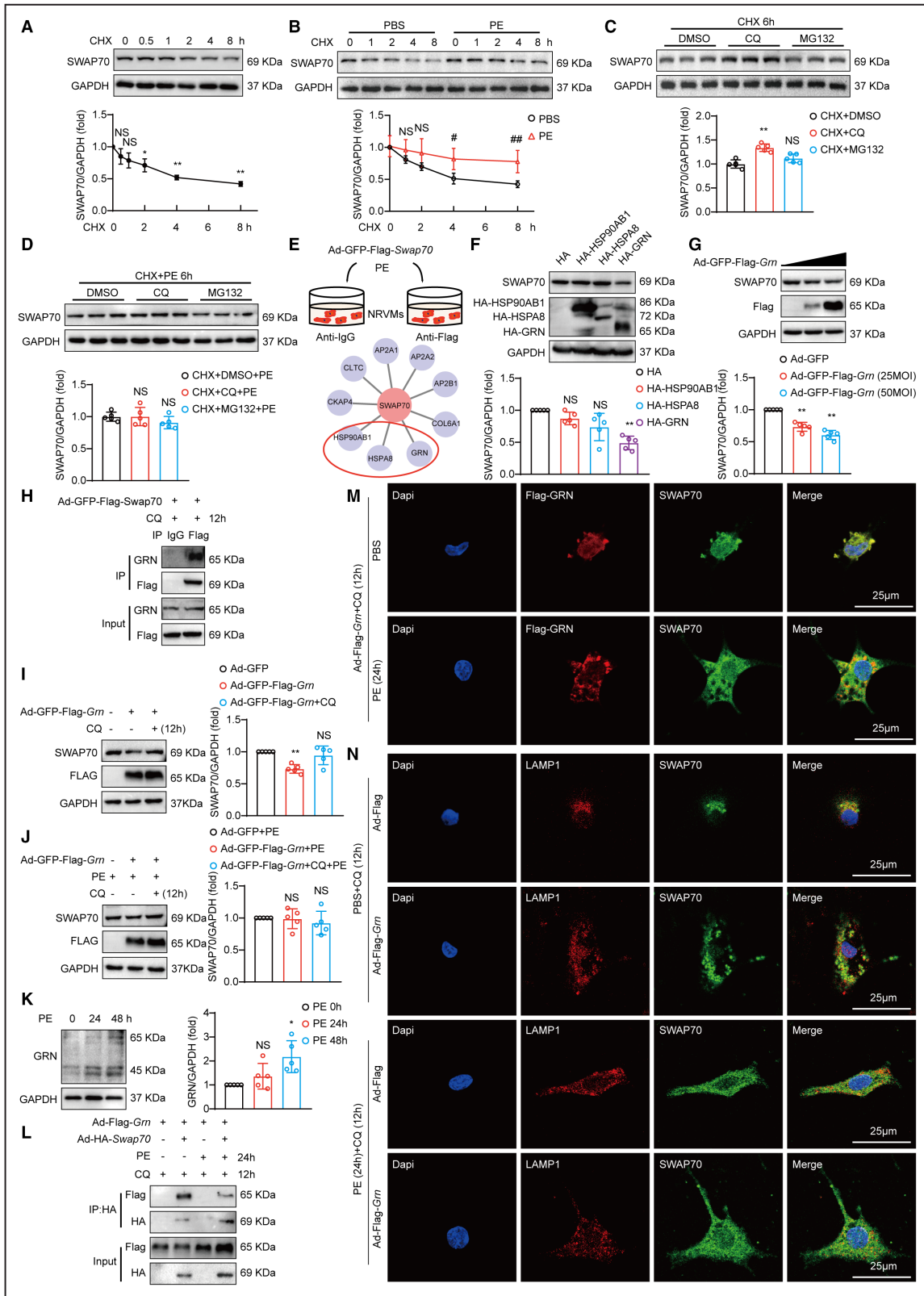
All animal experiments were approved by the Institutional Animal Care and Use Committee of the Zhongnan Hospital of Wuhan University (ZN2021201). The mice received humane care in accordance with the *Guide for the Care and Use of Laboratory Animals* published by the National Institutes of Health. C57BL/6 male mice (weight, 25.5–27 g; age, 9–11 weeks) were fed in a pathogen-free environment (temperature, 22–24 °C; humidity, 40%–70%; and 12-hour light cycle). The animals were in good health before transverse aortic constriction (TAC) or sham surgery and had access to food and water ad libitum. All data were obtained during this period, and operations and subsequent analyses were performed in a blinded manner.

Statistical Analysis

All data were analyzed using SPSS (IBM, Armonk, NY) and expressed as mean±SD. Data with normal

Figure 2. Hypertrophic increase in SWAP70 is connected with the inhibition of lysosomal degradation regulated by granulin precursor.

A, Immunoblotting and quantitation of SWAP70 protein levels in NRVMs added with CHX (25 μmol/L) for indicated time points (n=5 independent experiments) (NS: left, $P=0.54$; right, $P=0.21$). **B**, Immunoblotting and quantitation of SWAP70 protein levels in NRVMs added with CHX (25 μmol/L) for indicated time points with or without the stimulation of PE (50 μmol/L) (n=5 independent experiments) (NS: left, $P=0.09$; right, $P=0.08$). **C**, The protein expression and quantitation results of SWAP70 in NRVMs treated with DMSO, CQ (50 μmol/L), or MG132 (50 μmol/L) in the presence of CHX (25 μmol/L) for 6 hours (n=5 independent experiments) (NS: $P=0.15$). **D**, The protein expression and quantitation results of SWAP70 in NRVMs treated with DMSO, CQ (50 μmol/L), or MG132 (50 μmol/L) in the presence of CHX (25 μmol/L) and PE (50 μmol/L) for 6 hours (n=5 independent experiments) (NS: left, $P=1.00$; right, $P=0.60$). **E**, Upper, mode pattern showed that NRVMs were infected with Ad-GFP-Flag-*Swap70* and treated with PE (50 μmol/L, 48 hours), and then incubated with anti-IgG or Anti-Flag for mass spectrometry. Below, mass spectrometry screened the lysosomal related molecules and chose 3 of which according to its cellular function and localization. **F**, Immunoblotting and quantitation of SWAP70 protein levels in human embryonic kidney 293T cells transfected with indicated molecules (n=5 independent experiments) (NS: left, $P=0.24$; right, $P=0.28$). **G**, Immunoblotting and quantitation of SWAP70 protein levels in NRVMs infected with Ad-GFP-Flag-*Grn* adenovirus at different multiplicities of infection (n=5 independent experiments). **H**, CO-IP assays displayed the interaction between exogenous SWAP70 and endogenous GRN in NRVMs. **I**, Immunoblotting and quantitation of SWAP70 protein levels in NRVMs infected with or without Ad-GFP-Flag-*Grn* adenovirus in the presence or absence of CQ (25 μmol/L) for 12 hours (n=5 independent experiments) (NS: $P=0.82$). **J**, Immunoblotting and quantitation of SWAP70 protein levels in NRVMs accompanied with indicated adenovirus and drugs (n=5 independent experiments) (NS: Left, $P=1.00$; Right, $P=1.00$). **K**, Immunoblotting and quantitation of GRN protein levels in NRVMs with PE (50 μmol/L) treatment at indicated time points (n=5 independent experiments) (NS: $P=0.50$). **L**, CO-IP assays performed the interaction between SWAP70 and GRN in NRVMs accompanied with indicated adenoviruses and treatments. **M**, Representative immunofluorescence images of the colocalization of endogenous SWAP70 and exogenous GRN in NRVMs added with CQ (25 μmol/L, 12 hours) and Ad-Flag-*Grn* adenoviruses in the presence or absence of PE (50 μmol/L, 24 hours). **N**, Representative immunofluorescence images of the colocalization of endogenous SWAP70 and lysosome marker LAMP1 in NRVMs accompanied with indicated adenoviruses and treatments. Scale bar, 25 μm. Data are shown as mean±SD. Student *t*-test (**B**) and 1-way ANOVA with Bonferroni's post hoc analysis (**C**, **D**, **G**, and **J**) or with Tamhane T2 post hoc test (**A**, **F**, **I**, **K**) were used. * $P<0.05$; ** $P<0.01$ for indicated group vs control group. # $P<0.05$; ## $P<0.01$ for PE group vs PBS group. NS for indicated group vs control group or PE group vs PBS group (**B**). CHX indicates cycloheximide; CO-IP, coimmunoprecipitation; CQ, chloroquine; GRN, granulin precursor; LAMP1, lysosomal associated membrane protein 1; NRVMs, neonatal rat ventricular myocytes; NS, no significance; PE, phenylephrine; and SWAP70, switch-associated protein 70.



distribution were subjected to Student's *t*-test or 1-way ANOVA to evaluate differences between 2 or multiple groups, respectively. The Bonferroni post hoc test

(assuming homogeneity of variance) or Tamhane T2 post hoc test (assuming heterogeneity of variance) was applied for correction in 1-way ANOVA. Data with

nonnormal distribution were subjected to the Kruskal–Wallis nonparametric statistical test. Differences were considered statistically significant at $P < 0.05$.

RESULTS

SWAP70 Protein Level Is Increased in Response to Hypertrophic Stimuli

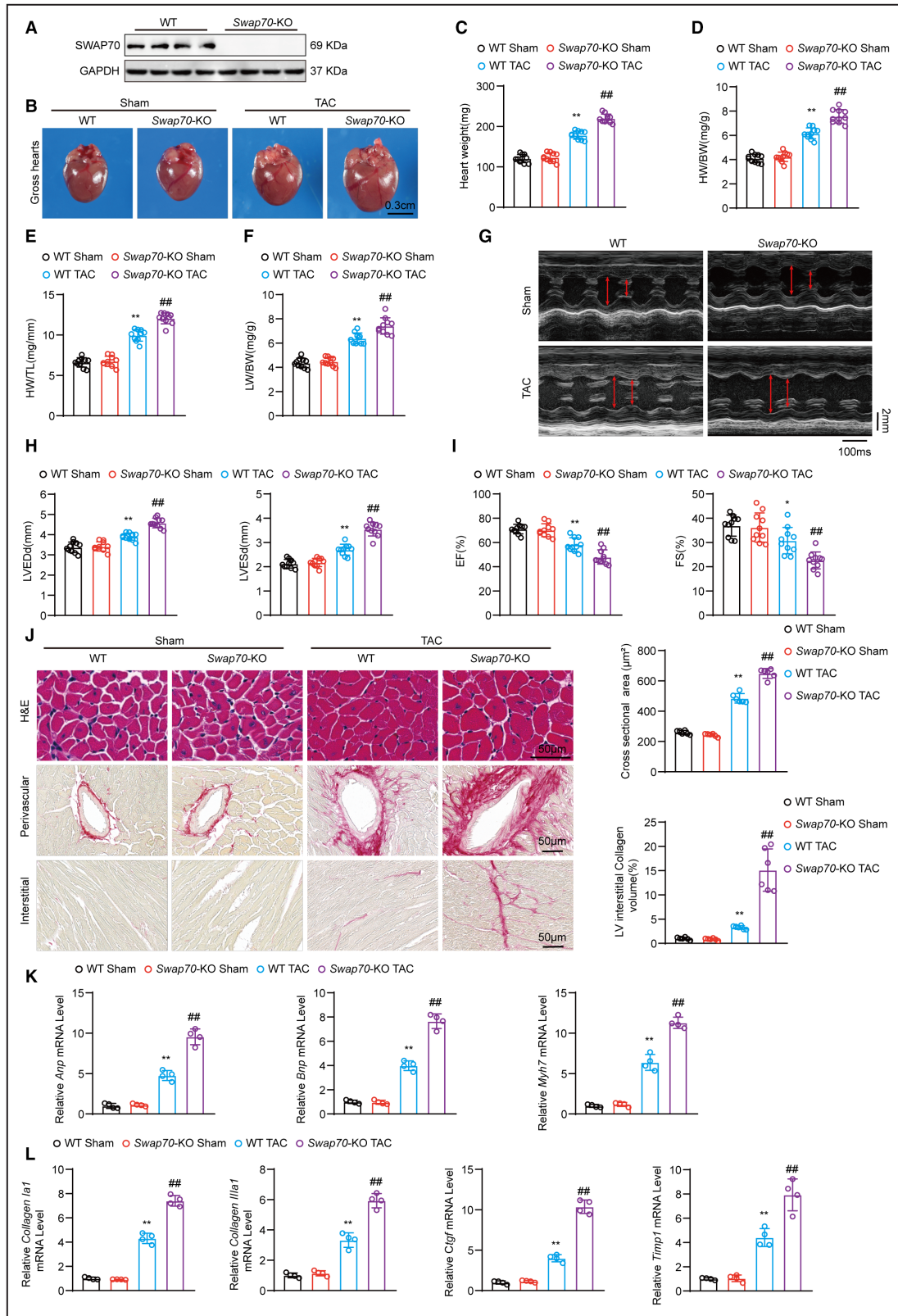
To determine changes in SWAP70 expression in response to hypertrophic stimuli, we first measured SWAP70 expression in human failing heart tissues through immunohistochemical staining, Western blot, and quantitative real-time polymerase chain reaction analyses. Western blot analysis revealed that SWAP70 protein expression was significantly higher in samples extracted from the above human failing heart tissues than that in normal tissues, and this result correlated well with the changes in heart failure markers (ANP [atrial natriuretic peptide], BNP [B-type natriuretic peptide], and β -myosin-heavy-chain [MYH7/ β -MHC]) (Figure 1A). However, the mRNA expression of SWAP70 showed no significant changes in these tissues (Figure 1B), suggesting that the increased protein expression of SWAP70 was posttranscriptionally regulated. Consistent with Western blot, immunohistochemical staining indicated higher protein levels of SWAP70 in failing heart tissues from patients with either hypertrophic cardiomyopathy or dilated cardiomyopathy than in normal tissues (Figure 1C). In addition, we detected the protein expression of SWAP70 in *in vivo* and *in vitro* cardiac hypertrophic models. The protein expression of SWAP70 was increased in cardiac tissues after 4 weeks of TAC surgery or in isolated primary NRVMs after 24 hours of phenylephrine treatment, and these changes were consistent with the changes in ANP, BNP, and MYH7 (Figure 1D and 1F). However, *Swap70* mRNA levels showed minimal changes at indicated times during the *in vitro* and *in vivo* experiments (Figure 1E and 1G). These data revealed that SWAP70 protein expression was increased posttranscriptionally under hypertrophic stimuli.

Hypertrophic Increase in SWAP70 Is Connected With the Inhibition of Lysosomal Degradation Regulated by Granulin Precursor

To identify the source of increased SWAP70 protein in a hypertrophic environment, we first explored the half-life of SWAP70 in NRVMs, and results showed that the half-life of SWAP70 was ≈ 4 hours in the presence of protein translation inhibitor cycloheximide (Figure 2A). Further experiments in NRVMs showed that hypertrophic stimulation (phenylephrine treatment) significantly prolonged the half-life of SWAP70, indicating that the high protein expression of SWAP70 may be ascribed to its reduced protein degradation under hypertrophic stimuli (Figure 2B). As shown in Figure 2C, SWAP70 protein expression was increased in the NRVMs treated with the lysosomal degradation inhibitor chloroquine but not obviously changed in the cells treated with the proteasome degradation inhibitor MG132, indicating that SWAP70 degradation was lysosome dependent under normal conditions. However, SWAP70 expression showed no obvious change after the treatment with chloroquine or MG132 in the presence of cycloheximide and phenylephrine compared with the control group (Figure 2D), suggesting that the increased SWAP70 protein expression after phenylephrine treatment can be ascribed to its reduced lysosomal degradation. To explore the possible upstream molecule(s) involved in the lysosomal regulation of SWAP70 protein expression, we performed protein mass spectrometry, intersected it with a subcellular localization database (<https://compartments.jensenlab.org/Search>) by bioinformatics to find the molecules that can colocalize with lysosomes (9 molecules remained after this step), and finally used a protein database (<https://www.uniprot.org>) to inquire about the function of these 9 molecules and gained 3 of them that were reported to involve in the regulation of molecular degradation^{31–33} (Figure 2E). Further experiments in human embryonic kidney 293T cells transfected with the indicated molecules suggested that granulin precursor (GRN)

Figure 3. *Swap70* deficiency accelerates pathological cardiac hypertrophy.

A, The protein expression of SWAP70 in mice heart tissues from WT or *Swap70*-KO mice ($n=4$). **B**, Representative heart size of mice from indicated groups. Scale bar, 0.3 cm. **C** through **F**, Heart weight, heart/body weight ratios, heart weight/tibia length ratios, and lung/body weight ratios in WT and *Swap70*-knockout mice at 4 weeks after sham or TAC surgery ($n=10$). **G**, Representative echocardiography images of indicated groups ($n=10$). **H** and **I**, Echocardiography assessed the parameters of LVEDd, LVESd, EF, and FS in WT or *Swap70*-KO mice at 4 weeks after sham or TAC surgery ($n=10$). **J**, Representative H&E (upper left) and picrosirius red (lower left) staining in the heart tissues from WT or *Swap70*-KO mice at 4 weeks after sham or TAC surgery. Scale bar, 50 μ m. Quantitative results of the average cross-sectional areas and left ventricular interstitial collagen volume is performed at the right ($n=6$). **K** and **L**, Relative mRNA levels of hypertrophy (*Anp*, *BNP*, *Myh7*), and fibrosis (*collagen $\alpha 1$* , *collagen $\text{III} \alpha 1$* , *Ctgf*, *Timp1*) related genes in mice heart tissues from indicated groups ($n=4$). Data are shown as mean \pm SD. One-way ANOVA with Bonferroni's post hoc analysis (**C** through **F**, **H** through **L**) or with Tamhane T2 post hoc test (left ventricular interstitial collagen volume in **J**, *collagen $\alpha 1$* and *Ctgf* in **L**) were used. * $P < 0.05$; ** $P < 0.01$ for WT TAC group vs WT sham group. ## $P < 0.01$ for *Swap70*-KO TAC group vs WT TAC group. ANP indicates atrial natriuretic peptide; BNP, B-type natriuretic peptide; Ctgf, connective tissue growth factor; EF, ejection fraction; FS, fractional shortening; H&E, hematoxylin–eosin; LVEDd, left ventricular end-diastolic systolic diameter; LVESd, left ventricular end-systolic diameter; MYH7, β -myosin-heavy-chain; SWAP70, switch-associated protein 70; *Swap70*-KO, *Swap70*-knockout; TAC, transverse aortic constriction; *Timp1*, tissue inhibitor of metalloproteinase 1; and WT, wild-type.



regulated the lysosomal degradation of SWAP70 (Figure 2F). To confirm this finding, we infected NRVMs with *Grn* adenovirus at different multiplicities of infection. Results showed that SWAP70 protein expression

decreased with the increased expression of *Grn* adenovirus (Figure 2G). However, the mRNA level of *Swap70* did not change with GRN overexpression (Figure S1A). Further coimmunoprecipitation assay

in human embryonic kidney 293T cells and NRVMs revealed the interaction between SWAP70 and GRN (Figure 2H and Figure S1B). As shown in Figure 2I and 2J, chloroquine or phenylephrine treatment can restrain the GRN-regulated decrease in SWAP70 protein expression. Interestingly, analysis revealed that hypertrophic stimuli did not downregulate the protein expression of GRN or its 45-kDa degradation product in NRVMs (Figure 2K). Both endogenous and exogenous upregulation of GRN protein could not lead to the downregulation of SWAP70 expression under stimulation conditions, suggesting that the degradation of SWAP70 mediated by GRN may be altered under hypertrophic stimuli. Considering that GRN itself has no enzymatic activity, we speculated that the interaction between SWAP70 and GRN changed under hypertrophic stimuli. Then, coimmunoprecipitation and immunofluorescence analyses revealed that GRN and SWAP70 showed decreased interaction and colocalization in the phenylephrine group (Figure 2L, 2M, and Figure S1C). Moreover, immunofluorescence showed that GRN increased the colocalization of SWAP70 and lysosomal marker lysosomal associated membrane protein 1, which was suppressed by phenylephrine treatment (Figure 2N and Figure S1D). Taken together, these results suggest that lysosomes contribute to the upregulation of SWAP70 protein expression under hypertrophic stimuli, and GRN participates in the lysosomal regulation of SWAP70.

Swap70 Deficiency Accelerates Pathological Cardiac Hypertrophy

Swap70 knockout mice were generated (Figure S2A), and experimental pathological cardiac hypertrophy was induced by TAC surgery to evaluate the impact of SWAP70 on pathological cardiac hypertrophy. The efficiency of *Swap70* deletion was verified using Western blot (Figure 3A). Before surgery, mice were measured and found no difference in weight, heart rate, blood pressure, and blood velocity between different genotypes (Figure S2B through S2D). At 4 weeks after TAC surgery, the heart rate, blood velocity, and pressure gradient showed no difference between *Swap70* knockout and wild-type (WT) mice (Figure S2E through S2G), while the *Swap70* knockout mice displayed significantly increased heart size, heart weight, heart/body weight ratios, heart weight/tibia length ratios, and lung/body weight ratios compared with the WT mice (Figure 3B through 3F). Ultrasonic measurements of the left ventricular end-systolic diameter and left ventricular end-diastolic diameter showed similar trends (Figure 3G and 3H). Meanwhile, the ejection fraction and fractional shortening were lower in the *Swap70* knockout mice than those in the WT mice after TAC surgery (Figure 3I). Hematoxylin–eosin

staining showed that the cross-sectional area of cardiomyocytes from the *Swap70* knockout mice was obviously larger than that of cardiomyocytes from the WT mice under hypertrophic stimuli. Moreover, *Swap70* deficiency aggravated the perivascular and interstitial fibrosis of the hypertrophic heart (Figure 3J). Corresponding to the hematoxylin–eosin and picrosirius red staining, hypertrophic and fibrosis phenotypes were accompanied by the upregulation of hypertrophic genes (*Anp*, *Bnp*, and *Myh7*) and fibrotic genes (*collagen 1 α 1*, *collagen 3 α 1*, connective tissue growth factor [*Ctgf*], tissue inhibitor of metalloproteinase 1 [*Timp1*]) in the *Swap70* knockout mice compared with the WT mice under hypertrophic stimuli (Figure 3K and 3L). However, inflammatory genes (insulin 6 [*Ii-6*], *Il-1b*, tumor necrosis factor α [*Tnfa*]) showed no difference between *Swap70* knockout mice and WT mice (Figure S2H). Collectively, these results demonstrated that *Swap70* deficiency accelerated pathological cardiac hypertrophy.

Swap70 Overexpression Suppresses the Progression of Cardiomyocyte Hypertrophy

NRVMs were isolated and treated with phenylephrine to investigate the effect of SWAP70 on simulated cardiomyocyte hypertrophy. Knockdown or overexpression of *Swap70* was induced using adenoviruses containing *Swap70* short hairpin RNA or *Swap70*. Data showed that the NRVMs with *Swap70* knockdown showed higher protein and mRNA expression levels of hypertrophic markers ANP, BNP, and MYH7 than the control group under hypertrophic stimuli (Figure 4A and 4B). Consistently, the NRVMs with *Swap70* knockdown had larger cardiomyocyte areas than the control group under hypertrophic stimuli (Figure 4C). Meanwhile, the NRVMs with *Swap70* overexpression showed lower expression of hypertrophic markers and smaller cardiomyocyte areas than the control group following phenylephrine treatment (Figure 4D through 4F). Taken together, these data indicated that *Swap70* overexpression suppressed the progression of cardiomyocyte hypertrophy.

SWAP70 Alleviates the Activation of the Transforming Growth Factor β -Activated Kinase 1—c-Jun N-Terminal Kinase 1/2-P38 Pathway in Response to Hypertrophic Stimuli

To investigate the possible downstream targets of SWAP70 in pathological cardiac hypertrophy, we utilized an RNA sequencing assay to compare the cardiac tissues from the *Swap70* knockout mice and control mice under pressure overload. Bioinformatic analysis

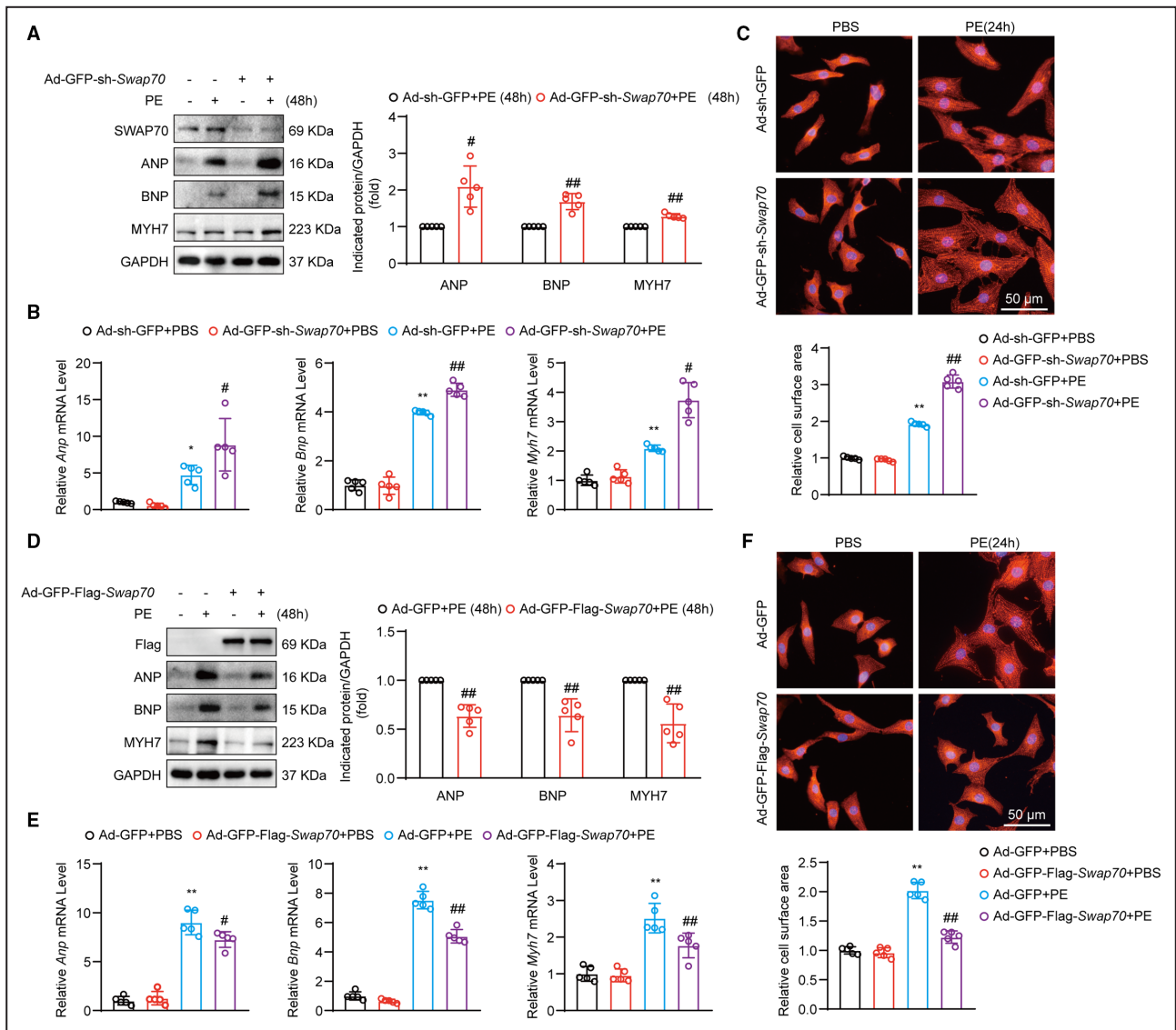


Figure 4. Swap70 overexpression suppresses the progression of cardiomyocyte hypertrophy.

A, Immunoblotting (left) and quantitation (right) of SWAP70, ANP, BNP, and MYH7 protein levels in NRVMs infected with Ad-GFP-sh-Swap70 or Ad-sh-GFP in the presence or absence of PE (50 μmol/L) for 48 hours (n=5 independent experiments). **B**, Relative mRNA levels of *Swap70* and hypertrophic marker genes (*Anp*, *Bnp*, and *Myh7*) in NRVMs from indicated groups (n=5 independent experiments). **C**, Representative immunofluorescence images (upper) of NRVMs infected with Ad-GFP-sh-Swap70 or Ad-sh-GFP adenovirus in the presence or absence of PE (50 μmol/L) for 24 hours and stained with α-actinin. Scale bar, 50 μm. Quantitative results (below) of the cardiomyocyte surface area from indicated groups (n=5 independent experiments). **D**, Immunoblotting (left) and quantitation (right) of SWAP70, ANP, BNP, MYH7 protein levels in NRVMs infected with Ad-GFP-Flag-Swap70 or Ad-GFP in the presence or absence of PE (50 μmol/L) for 48 hours (n=5 independent experiments). **E**, Relative mRNA levels of *Swap70* and hypertrophic marker genes (*Anp*, *Bnp*, and *Myh7*) in NRVMs from indicated groups (n=5 independent experiments). **F**, Representative immunofluorescence images (upper) of NRVMs infected with Ad-GFP-Flag-Swap70 or Ad-GFP adenovirus in the presence or absence of PE (50 μmol/L) for 24 hours and stained with α-actinin. Scale bar, 50 μm. Quantitative results (below) of the cell surface area from indicated groups (n=5 independent experiments). Data are shown as mean±SD. Student *t*-test (**A**, **D**) and 1-way ANOVA with Bonferroni's post hoc analysis (**B**, **E**, **F**) or with Tamhane T2 post hoc test (mRNA level of *Myh7* in **B**, **C**) were used. **P*<0.05; ***P*<0.01 for GFP PE group vs GFP PBS group. #*P*<0.05; ##*P*<0.01 for *Swap70* overexpression/knockdown PE group vs GFP PE group. ANP indicates atrial natriuretic peptide; BNP, B-type natriuretic peptide; MYH7, β-myosin-heavy-chain; NRVMs, neonatal rat ventricular myocytes; PE, phenylephrine; and SWAP70, switch-associated protein 70.

showed that differentially expressed genes were mainly related to fibrosis, heart function, and protein processing (Figure 5A through 5C). Kyoto Encyclopedia of Genes

and Genomes pathway enrichment analysis indicated that the MAPK pathway was significantly changed by *Swap70* deficiency (Figure 5D). Our previous research

found that among some of the upstream molecules of the MAPK pathway, transforming growth factor β -activated kinase 1 (TAK1) showed the strongest interaction with SWAP70.¹⁹ We examined the activation of

TAK1 and downstream c-Jun N-terminal kinase (JNK) 1/2-P38 molecules in hypertrophic mice or NRVMs and found that *Swap70* deficiency or knockdown aggravated the phosphorylation of these molecules and

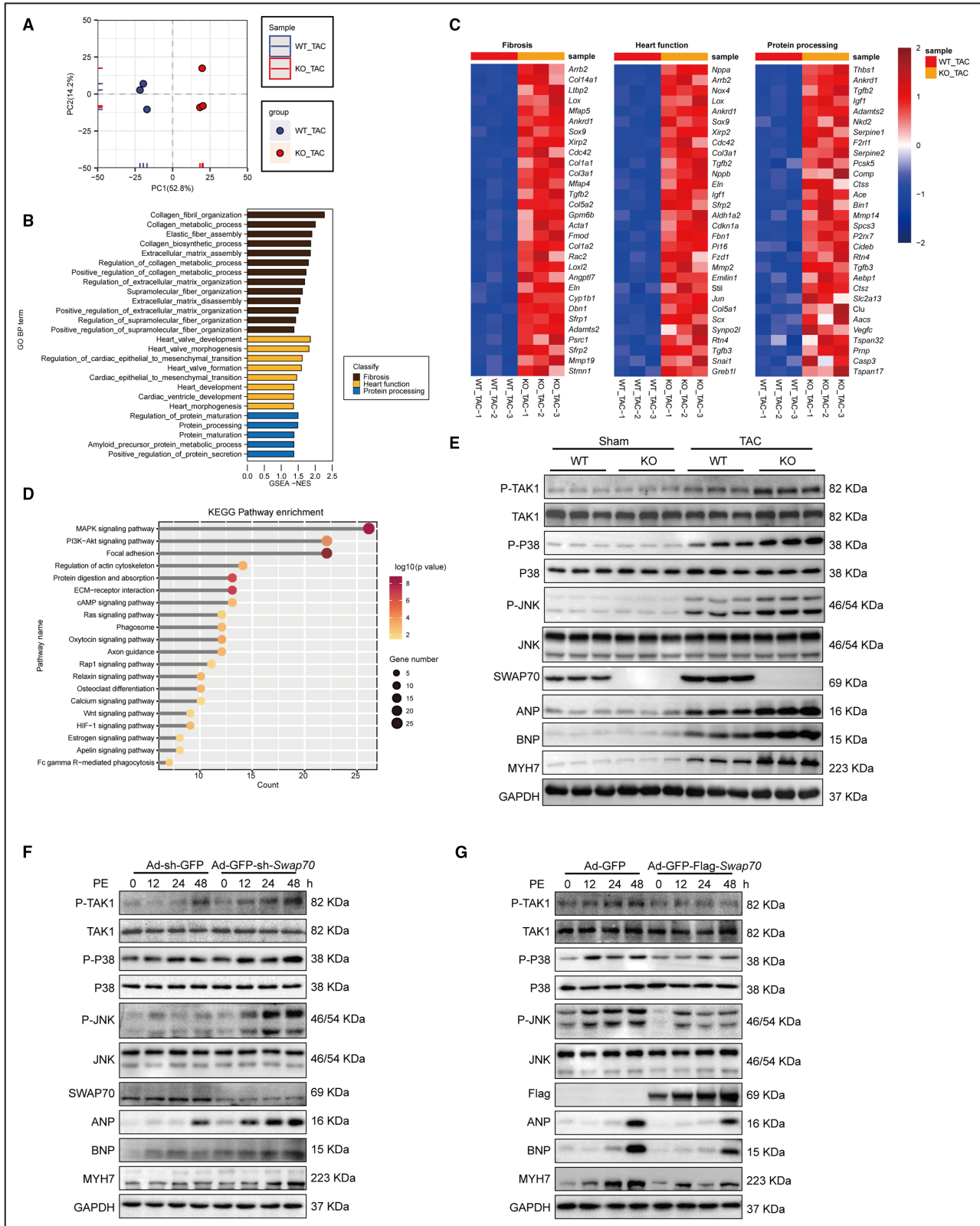


Figure 5. SWAP70 alleviates the activation of the TAK1-JNK1/2-P38 pathway in response to hypertrophic stimuli.

A, Hierarchical clustering analysis performed the global sample distribution profiles between WT mice and *Swap70*-KO mice under TAC surgery based on the RNA sequencing (RNA-seq, $n=3$). **B**, Gene set enrichment analysis of molecular events involved in fibrosis, heart function, and protein processing in RNA-seq data. **C**, Heatmaps about the significantly altered genes concerned with cardiac hypertrophy. **D**, Kyoto Encyclopedia of Genes and Genomes pathway enrichment about the significantly altered pathways according to the RNA-seq data. **E**, Immunoblotting analysis of phosphorylation and total TAK1, P38, JNK1/2 proteins in mice heart samples from indicated groups, hypertrophic marker proteins (ANP, BNP, and MYH7) were used to assess the severity of the hypertrophy ($n=4$). **F**, Immunoblotting analysis of phosphorylation and total TAK1, P38, JNK1/2 proteins in NRVMs infected with indicated adenovirus and stimulated with PE (50 $\mu\text{mol/L}$) for a time gradient, hypertrophic marker proteins (ANP, BNP, and MYH7) were used to assess the severity of the hypertrophy ($n=4$ independent experiments). **G**, Immunoblotting analysis of phosphorylation and total TAK1, P38, JNK1/2 proteins level in NRVMs infected with Ad-GFP or Ad-GFP-Flag-*Swap70* and stimulated with PE (50 $\mu\text{mol/L}$) for a time gradient, hypertrophic marker proteins (ANP, BNP, and MYH7) were used to assess the severity of the hypertrophy ($n=4$ independent experiments). ANP indicates atrial natriuretic peptide; BNP, B-type natriuretic peptide; JNK, c-Jun N-terminal kinase; MYH7, β -myosin-heavy-chain; NRVMs, neonatal rat ventricular myocytes; PE, phenylephrine; *Swap70*-KO, *Swap70*-knockout; TAK1, transforming growth factor β -activated kinase 1; and WT, wild-type.

accentuated the hypertrophic phenotype of the myocardium in *in vitro* and *in vivo* experiments (Figure 5E and 5F). Nevertheless, these effects were suppressed in the NRVMs with *Swap70* overexpression (Figure 5G). Moreover, we detected some landmark proteins in the phosphatidylinositol 3-kinases–protein kinase B pathway found in sequencing analysis and in the nuclear factor kappa-B pathway reported before that may be influenced by SWAP70.¹⁸ Results showed that *Swap70* knockdown/overexpression showed no influence on the phosphorylation of protein kinase B and $\text{I}\kappa\text{-}\beta$ kinase (Figure S3). These results indicated that *Swap70* deficiency promotes the activation of MAPK pathway and the progression of pathological cardiac hypertrophy.

SWAP70 Regulates Cardiomyocyte Hypertrophy by Suppressing the TAK1–Transforming Growth Factor β -Activated Kinase 1 Binding Protein 1 Interaction

To confirm whether SWAP70-mediated cardioprotective effects are dependent on TAK1 under hypertrophic stimuli, we analyzed the relationship between SWAP70 and TAK1 and found that SWAP70 colocalized with TAK1 in the cytoplasm of NRVMs (Figure 6A). Further immunoprecipitation assays showed that SWAP70 interacted with endogenous TAK1 in the NRVMs under hypertrophic stimuli (Figure 6B). As in our previous report, TAK1 interacts with the N-terminals (1–192) of SWAP70.¹⁹ We established N-terminal missing adenovirus (193–585) of *Swap70* and found that SWAP70 (193–585) could not interact with endogenous TAK1 under hypertrophic stimuli (Figure 6C). Further experiment found that *Swap70* (WT) instead of *Swap70* (193–585) inhibited the phosphorylation of TAK1 and downstream JNK1/2-P38 molecules, sequentially suppressing the progression of cardiomyocyte hypertrophy (Figure 6D). The expression of myocardial markers (ANP, BNP, and MYH7) showed that *Swap70* (193–585) failed to inhibit cardiac injury in a hypertrophic environment (Figure 6D and 6E). The α -actinin staining

indicative of cardiomyocyte area showed similar results (Figure 6F). Moreover, we previously discovered that SWAP70 could restrain the activation of TAK1 by inhibiting the interaction of TAK1 and transforming growth factor β -activated kinase 1 binding protein 1 (TAB1),¹⁹ which is essential for the activation of TAK1.³⁴ We established Ad-GFP-Flag-*Tab1* adenovirus and found that SWAP70 could restrain the activation of TAK1-JNK1/2-P38 signaling caused by TAB1 overexpression, thus suppressing the expression of hypertrophic markers and inhibiting cardiomyocyte hypertrophy (Figure S4). These data revealed that SWAP70 interacted with TAK1 and that SWAP70 overexpression mediated cardioprotective effects by suppressing the interaction between TAB1 and TAK1.

Inhibiting the Activation of TAK1 Rescues the Aggravated Cardiomyocyte Hypertrophy Induced by *Swap70* Knockdown

Considering that TAK1 activation is essential in the progression of cardiomyocyte hypertrophy, we used the TAK1 inhibitor 5Z-7-oxozeaenol to explore the role of TAK1 activity in the progression of cardiomyocyte hypertrophy following *Swap70* knockdown. Results showed that the phosphorylation of downstream JNK1/2-P38 decreased with the suppression of TAK1 activity (Figure 7A). At this point, the protein and mRNA expression of myocardial markers (ANP, BNP, and MYH7) upregulated by *Swap70* knockdown were countered by 5Z-7-oxozeaenol (Figure 7A and 7C). Immunofluorescence staining of α -actinin revealed a similar trend in the cardiomyocyte surface area (Figure 7B). In addition, we established Ad-GFP-sh-*Tak1* adenovirus to further examine the functions of TAK1 in the progression of cardiomyocyte hypertrophy regulated by SWAP70 (Figure 7D and 7E). Similar to the results obtained with 5Z-7-oxozeaenol, *Tak1* knockdown significantly decreased the activity of TAK1 and downstream phosphorylation of JNK1/2 and P38

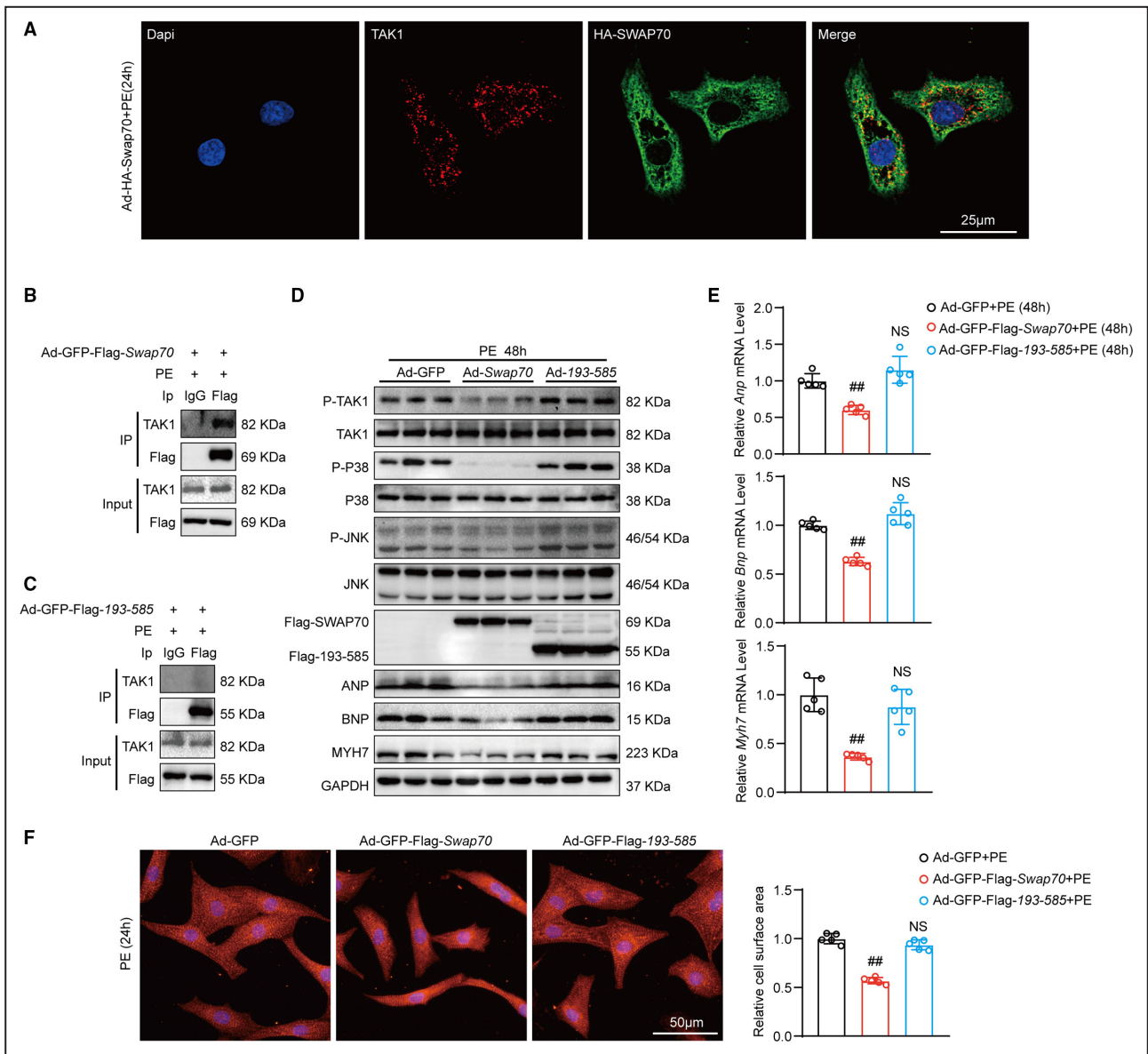


Figure 6. SWAP70 regulates cardiomyocyte hypertrophy by interacting with TAK1.

A, Representative immunofluorescence images of the colocalization of HA-tagged SWAP70 and endogenous TAK1 in NRVMs infected with Ad-HA-Swap70 adenovirus in the presence of PE (50 µmol/L) for 24 hours. Scale bar, 25 µm. **B**, CO-IP assays displayed the interaction between endogenous TAK1 and Flag-tagged SWAP70 in NRVMs. **C**, CO-IP assays displayed the interaction between endogenous TAK1 and Flag-tagged SWAP70 (193–585) in NRVMs. **D**, Immunoblotting analysis of phosphorylation and total TAK1, P38, JNK1/2 proteins in NRVMs infected with indicated adenoviruses and stimulated with PE (50 µmol/L) for 48 hours, hypertrophic marker proteins (ANP, BNP, and MYH7) were used to assess the severity of the hypertrophy (n=5 independent experiments). **E**, Relative mRNA levels of hypertrophic marker genes (*Anp*, *Bnp*, and *Myh7*) in NRVMs from indicated groups (n=5 independent experiments) (NS: high, $P=0.25$; middle, $P=0.08$; low, $P=0.65$). **F**, Representative immunofluorescence images (left) of NRVMs infected with indicated adenovirus in the presence of PE (50 µmol/L) for 24 hours and stained with α -actinin. Scale bar, 50 µm. Quantitative results (right) of the cell surface area from indicated groups (n=5 independent experiments) (NS: $P=0.15$). Data are shown as mean±SD. One-way ANOVA with Bonferroni’s post hoc analysis (**E**, **F**) or with Tamhane T2 post hoc test (mRNA levels of *Myh7* in **E**) were used. ## $P<0.01$ for indicated group vs control group. NS for indicated group vs control group. ANP indicates atrial natriuretic peptide; BNP, B-type natriuretic peptide; CO-IP, coimmunoprecipitation; JNK, c-Jun N-terminal kinase; MYH7, β -myosin-heavy-chain; NRVMs, neonatal rat ventricular myocytes; NS, no significance; PE, phenylephrine; SWAP70, switch-associated protein 70; and TAK1, transforming growth factor β -activated kinase 1.

molecules, thus reversing the exacerbation of cardiomyocyte hypertrophy induced by *Swap70* knockdown following phenylephrine treatment (Figure 7F through

7H). These results demonstrated that SWAP70 protected against cardiomyocyte hypertrophy by inhibiting the activation of TAK1.

DISCUSSION

The salient findings from our present study revealed that *Swap70* deficiency could promote the progression of cardiac hypertrophy. Under hypertrophic stimuli, SWAP70 was less degraded by lysosome through an interaction change between GRN and SWAP70. Further gain- and loss-of-function approaches showed that *Swap70* overexpression inhibited the progression of cardiomyocyte hypertrophy in a TAK1-dependent manner by suppressing the TAK1-TAB1 interaction and subsequent activation of MAPK pathway.

Previous studies on SWAP70 mainly focused on immunity, tumor progression, and erythropoiesis.^{35–41} SWAP70 interacts with F-actin, interferon regulatory factor 4, and Rac1, thus participating in the membrane ruffling,³⁷ actin rearrangements,³⁸ phagocytosis,³⁹ micropinocytosis,⁴⁰ and differentiation⁴¹ of cells. SWAP70 seems to allow cells to evolve into more dynamic forms and functions. However, its role in pathological cardiac hypertrophy remains unclear. In the present study, SWAP70 protein expression was significantly upregulated in hypertrophic cardiomyocytes, and *Swap70* overexpression delayed the progression of cardiac hypertrophy. This result indicated that the hypertrophy-induced upregulation of SWAP70 protein was a compensatory but insufficient response to cardiac injury. Gain- and loss-of-function studies revealed the protective effects of SWAP70 against the progression of pathological cardiac hypertrophy. Intriguingly, *Swap70* deletion or overexpression alone did not exert significant effects on the mice or primary cardiomyocytes, indicating that SWAP70 mainly works under pathological conditions.

On the other hand, the mRNA levels of *Swap70* showed no significant change both in in vitro and in vivo experiments. Further exploration revealed that lysosomes may participate in the accumulation of SWAP70 in a hypertrophic environment. Through immunoprecipitation mass spectrometry, we identified an upstream regulatory molecule that mediates the lysosomal degradation of SWAP70, called GRN, which was reported to regulate lysosomal function by mediating the activity of lysosomal enzymes and trafficking of proteins to lysosomes.^{42,43} In the present study, GRN could downregulate the protein expression of SWAP70, while it was blocked under hypertrophic stimuli. However, similar to a previous report on age-related cardiac hypertrophy,⁴⁴ the present study revealed that the protein expression of GRN showed no decrease in NRVMs, indicating the regulation form between SWAP70 and GRN may be altered under hypertrophic stimuli. A previous study found that SWAP70 interacts with Rac1 under stimulation but not under normal conditions.³⁹ Another study reported that a mutant of SWAP70 can exist at the plasma membrane without any stimulation

while SWAP70 itself could not.⁴⁵ Similarly, our results showed an interaction change between SWAP70 and GRN in a hypertrophic environment. Thus, SWAP70 under normal or pathological conditions may have different configurations that influence the forms and functions of cells. In the present study, hypertrophic stimuli reduced the colocalization of SWAP70 with GRN or lysosomal marker lysosomal associated membrane protein 1. Hypertrophic stimuli possibly decreased the lysosomal degradation of SWAP70 by disrupting the interaction of SWAP70 with GRN. GRN at least partially participates in the maintenance of SWAP70 protein levels under normal conditions through the lysosomal degradation pathway. However, a more comprehensive study should be conducted to investigate the role of GRN in pathological cardiac hypertrophy with emphasis on SWAP70 regulation.

Through RNA sequencing, we found that the MAPK pathway, which has been reported to effectively influence the progression of pathological cardiac hypertrophy,^{10,46} played an important role in the progression of pathological cardiac hypertrophy mediated by *Swap70* deficiency. *Swap70* overexpression suppressed the progression of cardiac hypertrophy possibly by inhibiting the interaction between TAK1 and TAB1, which is essential for the activation of TAK1,³⁴ and further restrained the phosphorylation of TAK1 and downstream JNK1/2-P38 pathways. Similar to our previous research,¹⁹ SWAP70 derived from different cell types may have multifunctional roles in different disease models. However, there still remain some elusive places in the relationship between TAK1 and pathological cardiac hypertrophy. Previous studies in mice found that TAK1 expression is higher in embryos or neonate mice and decreases gradually before adulthood. Widespread hyperactivation of TAK1 leads to the death of mice attributable to hypertrophic cardiomyopathy within 2 weeks of birth.⁴⁷ Similar to our results, upregulation of TAK1 phosphorylation has been observed in stress hypertrophy models.⁴⁸ Meanwhile, another study reported that *Tak1* knockout mice under pressure overload show increased risk for cardiac hypertrophy and heart failure.⁴⁹ Therefore, the timing and extent of TAK1 activation are critical to its role in the heart. In the present study, restrained activation of TAK1 could inhibit the progression of cardiomyocyte hypertrophy caused by *Swap70* knockdown under pressure overload. We speculate that a low level of TAK1 activation may be beneficial for the inhibition of pathological cardiac hypertrophy regulated by *Swap70* knockdown. Moreover, it has been proved that TAK1 binds to the N-terminals of SWAP70.¹⁹ In the present study, N-terminal deletion of *Swap70* did not effectively inhibit the activation of TAK1, thus failing to protect against the progression of cardiac hypertrophy. This result indicates that *Swap70* overexpression restrained

the progression of cardiomyocyte hypertrophy in a TAK1-dependent manner.

There still exist some limitations in the present study. First, experiments with cardiac-specific *Swap70*

overexpression or knockout mice could further examine the protective effects of SWAP70 against the progression of pathological cardiac hypertrophy. Second, a use of human-induced pluripotent stem cells may

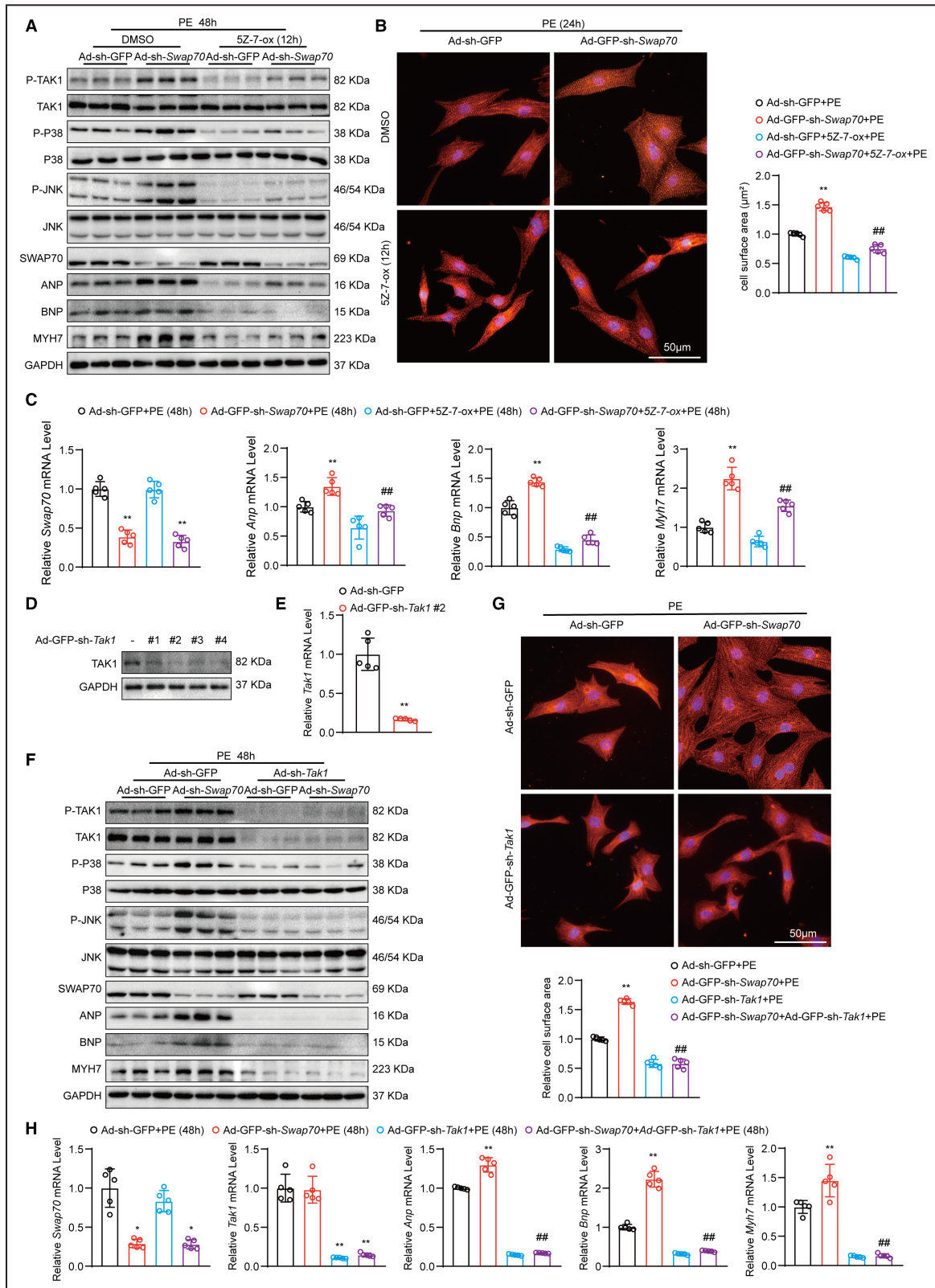


Figure 7. Inhibiting the activation of TAK1 rescues the aggravated cardiomyocyte hypertrophy induced by *Swap70* knockdown.

A, Immunoblotting analysis of phosphorylation and total TAK1, P38, JNK1/2 proteins in NRVMs infected with indicated adenoviruses and treated with DMSO or 5Z-7-oxozeaenol (100nmol/L, 12 hours) in the presence of PE (50 μmol/L, 48 hours), hypertrophic marker proteins (ANP, BNP, and MYH7) were used to assess the severity of the hypertrophy (n=5 independent experiments). **B**, Representative immunofluorescence images (left) of NRVMs infected with indicated adenovirus, treated with DMSO or 5Z-7-oxozeaenol (100nmol/L, 12 hours) in the presence of PE (50 μmol/L, 24 hours) and stained with α-actinin. Scale bar, 50 μm. Quantitative results (right) of the cell surface area from indicated groups (n=5 independent experiments). **C**, Relative mRNA levels of *Swap70* and hypertrophic marker genes (*Anp*, *BNP*, *Myh7*) in NRVMs from indicated groups (n=5 independent experiments). **D**, The protein expression of TAK1 in NRVMs after infection with Ad-GFP-sh-*Tak1* #1, #2, #3, or #4 adenovirus for 48 hours. **E**, Relative mRNA levels of *Tak1* in NRVMs after infection with Ad-GFP-sh-*Tak1* #2 for 48 hours (n=5 independent experiments) **F**, Immunoblotting analysis of phosphorylation and total TAK1, P38, JNK1/2 proteins in NRVMs infected with indicated adenoviruses and stimulated with PE (50 μmol/L) for 48 hours, hypertrophic marker proteins (ANP, BNP, and MYH7) were used to assess the severity of the hypertrophy (n=5 independent experiments). **G**, Representative immunofluorescence images (upper) of NRVMs infected with indicated adenovirus, treated with PE (50 μmol/L) for 24 hours and stained with α-actinin. Scale bar, 50 μm. Quantitative results (below) of the cell surface area from indicated groups (n=5 independent experiments). **H**, Relative mRNA levels of *Swap70*, *Tak1*, and hypertrophic marker genes (*Anp*, *BNP*, and *Myh7*) in NRVMs from indicated groups (n=5 independent experiments). Data are shown as mean±SD. Student *t*-test (**E**) and 1-way ANOVA with Bonferroni's post hoc analysis (**B**, **C**, **G**, mRNA levels of *Myh7* in **H**) or with Tamhane T2 post hoc test (**H**) were used. Kruskal-Wallis nonparametric statistical test (mRNA levels of *Tak1* in **H**) was used for nonnormal distribution data. **P*<0.05; ***P*<0.01 for indicated group vs control group. ##*P*<0.01 for indicated group vs sh-*Swap70* PE group. ANP indicates atrial natriuretic peptide; BNP, B-type natriuretic peptide; JNK, c-Jun N-terminal kinase; MYH7, β-myosin-heavy-chain; NRVMs, neonatal rat ventricular myocytes; PE, phenylephrine; and TAK1, transforming growth factor β-activated kinase 1.

help us better study the function of SWAP70 in hypertrophy and link the research to clinical applications. Third, if there exists a mutant isoform of the SWAP70

protein that can inhibit TAK1 activation and avoid lysosomal degradation simultaneously, it may be better for clinical application. We expect to further explore the

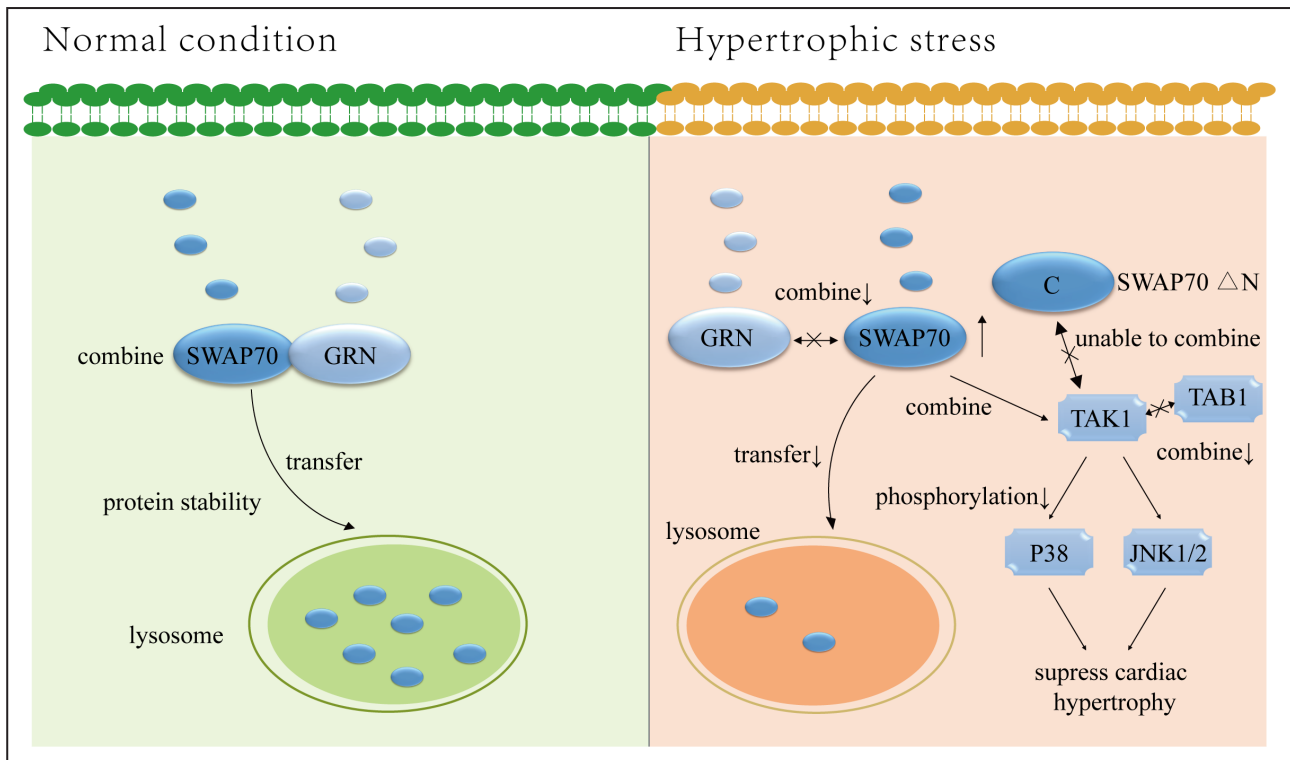


Figure 8. Schematic showing possible mechanisms underlying normal or hypertrophic environment associated with SWAP70.

Under normal conditions, SWAP70 is degraded by lysosomes mediated by GRN to maintain the balance of SWAP70 protein level, while hypertrophic stress reduces the binding of SWAP70 to GRN and thus decreases the lysosomal degradation of SWAP70, leads to the increased SWAP70 protein level, decreases the interaction between TAK1 and TAB1, inhibits the phosphorylation of TAK1-JNK 1/2-P38 signaling pathways, and finally suppresses cardiac hypertrophy. The phosphorylation inhibition of TAK1 by SWAP70 is dependent on its N-terminal interaction with TAK1. GRN indicates granulin precursor; JNK, c-Jun N-terminal kinase; SWAP70, switch-associated protein 70; TAB1, transforming growth factor β-activated kinase 1 binding protein 1; and TAK1, transforming growth factor β-activated kinase 1.

lysosomal regulation mechanism of SWAP70 in future studies and try to find a mutant of SWAP70 with an activated conformation to obtain a functional and structurally stable SWAP70 protein for clinical application.

CONCLUSIONS

Our data showed that SWAP70 was upregulated in primary cardiomyocytes, mice, and human heart tissues under pressure overload. In a disease state, the increase in SWAP70 protein expression may partly result from the GRN-mediated suppression of lysosomal degradation. *Swap70* overexpression alleviated the progression of cardiomyocyte hypertrophy by inhibiting the activation of TAK1 and downstream JNK1/2-P38 pathways. Reducing the activation of TAK1 could effectively alleviate cardiomyocyte hypertrophy aggravated by *Swap70* knockdown. SWAP70 interacted with TAK1 and decreased the TAK1-TAB1 interaction. *Swap70* overexpression restrained the progression of cardiomyocyte hypertrophy in a TAK1-dependent manner (Figure 8). This study revealed the regulation pattern of the expression and mechanism of SWAP70 under pathological conditions, which may provide a potential therapeutic target for the treatment of pathological cardiac hypertrophy.

ARTICLE INFORMATION

Received October 26, 2022; accepted February 20, 2023.

Affiliations

Department of Cardiovascular Surgery, Zhongnan Hospital of Wuhan University, Wuhan, China (Q.Q., W.Y., D.L., Y.L., H.S., D.D., K.D., C.L., J.L.); Hubei Provincial Engineering Research Center of Minimally Invasive Cardiovascular Surgery, Wuhan, China (W.Y., D.L., C.L., J.L.); Wuhan Clinical Research Center for Minimally Invasive Treatment of Structural Heart Disease, Wuhan, China (W.Y., D.L., C.L., J.L.); and Medical Science Research Centre, Zhongnan Hospital of Wuhan University, Wuhan, China (F.H.).

Acknowledgments

The authors thank the participants and staff involved in the study.

Sources of Funding

This work was supported by National Science Foundation of China (82170505), Key Research and Development Project of Hubei Provincial Department of Science and Technology (2020BCB053), and Talent Project of Zhongnan Hospital of Hubei Province (20220501).

Disclosures

None.

Supplemental Material

Data S1

REFERENCES

- Hall C, Gehmlich K, Denning C, Pavlovic D. Complex relationship between cardiac fibroblasts and cardiomyocytes in health and disease. *J Am Heart Assoc.* 2021;10:e19338. doi: 10.1161/JAHA.120.019338
- Chen QQ, Ma G, Liu JF, Cai YY, Zhang JY, Wei TT, Pan A, Jiang S, Xiao Y, Xiao P, et al. Neuraminidase 1 is a driver of experimental cardiac hypertrophy. *Eur Heart J.* 2021;42:3770–3782. doi: 10.1093/eurheartj/ehab347
- Shimizu I, Minamino T. Physiological and pathological cardiac hypertrophy. *J Mol Cell Cardiol.* 2016;97:245–262. doi: 10.1016/j.yjmcc.2016.06.001
- Wei J, Joshi S, Speransky S, Crowley C, Jayathilaka N, Lei X, Wu Y, Gai D, Jain S, Hoosien M, et al. Reversal of pathological cardiac hypertrophy via the MEF2-coregulator interface. *JCI Insight.* 2017;2:e91068. doi: 10.1172/jci.insight.91068
- Oka T, Akazawa H, Naito AT, Komuro I. Angiogenesis and cardiac hypertrophy: maintenance of cardiac function and causative roles in heart failure. *Circ Res.* 2014;114:565–571. doi: 10.1161/CIRCRESAHA.114.300507
- Tham YK, Bernardo BC, Ooi JY, Weeks KL, McMullen JR. Pathophysiology of cardiac hypertrophy and heart failure: signaling pathways and novel therapeutic targets. *Arch Toxicol.* 2015;89:1401–1438. doi: 10.1007/s00204-015-1477-x
- Nakamura M, Sadoshima J. Mechanisms of physiological and pathological cardiac hypertrophy. *Nat Rev Cardiol.* 2018;15:387–407. doi: 10.1038/s41569-018-0007-y
- Liu J, Li W, Deng KQ, Tian S, Liu H, Shi H, Fang Q, Liu Z, Chen Z, Tian T, et al. The E3 ligase TRIM16 is a key suppressor of pathological cardiac hypertrophy. *Circ Res.* 2022;130:1586–1600. doi: 10.1161/CIRCRESAHA.121.318866
- Deng KQ, Zhao GN, Wang Z, Fang J, Jiang Z, Gong J, Yan FJ, Zhu XY, Zhang P, She ZG, et al. Targeting transmembrane BAX inhibitor motif containing 1 alleviates pathological cardiac hypertrophy. *Circulation.* 2018;137:1486–1504. doi: 10.1161/CIRCULATIONAHA.117.031659
- Luo Y, Jiang N, May HI, Luo X, Ferdous A, Schiattarella GG, Chen G, Li Q, Li C, Rothermel BA, et al. Cooperative binding of E2S2 and NFAT links Erk1/2 and calcineurin signaling in the pathogenesis of cardiac hypertrophy. *Circulation.* 2021;144:34–51. doi: 10.1161/CIRCULATIONAHA.120.052384
- Bass-Stringer S, Tai C, McMullen JR. IGF1-PI3K-induced physiological cardiac hypertrophy: implications for new heart failure therapies, biomarkers, and predicting cardiotoxicity. *J Sport Health Sci.* 2021;10:637–647. doi: 10.1016/j.jshs.2020.11.009
- Deng KQ, Wang A, Ji YX, Zhang XJ, Fang J, Zhang Y, Zhang P, Jiang X, Gao L, Zhu XY, et al. Suppressor of IKKe is an essential negative regulator of pathological cardiac hypertrophy. *Nat Commun.* 2016;7:11432. doi: 10.1038/ncomms11432
- Bei Y, Wang L, Ding R, Che L, Fan Z, Gao W, Liang Q, Lin S, Liu S, Lu X, et al. Animal exercise studies in cardiovascular research: current knowledge and optimal design—a position paper of the committee on cardiac rehabilitation, Chinese Medical Doctors' Association. *J Sport Health Sci.* 2021;10:660–674. doi: 10.1016/j.jshs.2021.08.002
- Xiao J, Rosenzweig A. Exercise and cardiovascular protection: update and future. *J Sport Health Sci.* 2021;10:607–608. doi: 10.1016/j.jshs.2021.11.001
- Manni M, Ricker E, Pernis AB. Regulation of systemic autoimmunity and CD11c(+) Tbet(+) B cells by SWEF proteins. *Cell Immunol.* 2017;321:46–51. doi: 10.1016/j.cellimm.2017.05.010
- Shi L, Liu H, Wang Y, Chong Y, Wang J, Liu G, Zhang X, Chen X, Li H, Niu M, et al. SWAP-70 promotes glioblastoma cellular migration and invasion by regulating the expression of CD44s. *Cancer Cell Int.* 2019;19:305. doi: 10.1186/s12935-019-1035-3
- Shinohara M, Terada Y, Iwamatsu A, Shinohara A, Mochizuki N, Higuchi M, Gotoh Y, Ihara S, Nagata S, Itoh H, et al. SWAP-70 is a guanine-nucleotide-exchange factor that mediates signalling of membrane ruffling. *Nature.* 2002;416:759–763. doi: 10.1038/416759a
- Popovic J, Wellstein I, Pernis A, Jessberger R, Ocana-Morgner C. Control of GM-CSF-dependent dendritic cell differentiation and maturation by DEF6 and SWAP-70. *J Immunol.* 2020;205:1306–1317. doi: 10.4049/jimmunol.2000020
- Qian Q, Li Y, Fu J, Leng D, Dong Z, Shi J, Shi H, Cao D, Cheng X, Hu Y, et al. Switch-associated protein 70 protects against nonalcoholic fatty liver disease through suppression of TAK1. *Hepatology.* 2022;75:1507–1522. doi: 10.1002/hep.32213
- Chang YT, Shu CL, Lai JY, Lin CY, Chuu CP, Morishita K, Ichikawa T, Jessberger R, Fukui Y. SWAP-70 contributes to spontaneous transformation of mouse embryo fibroblasts. *Exp Cell Res.* 2016;345:150–157. doi: 10.1016/j.yexcr.2015.06.011
- Ripich T, Jessberger R. SWAP-70 regulates erythropoiesis by controlling alpha4 integrin. *Haematologica.* 2011;96:1743–1752. doi: 10.3324/haematol.2011.050468
- Garbe AI, Roscher A, Schuler C, Lutter AH, Glosmann M, Bernhardt R, Chopin M, Hempel U, Hofbauer LC, Rammelt S, et al. Regulation

- of bone mass and osteoclast function depend on the F-Actin modulator SWAP-70. *J Bone Miner Res.* 2012;27:2085–2096. doi: [10.1002/jbmr.1670](https://doi.org/10.1002/jbmr.1670)
23. Pearce G, Angeli V, Randolph GJ, Junt T, von Andrian U, Schnittler HJ, Jessberger R. Signaling protein SWAP-70 is required for efficient B cell homing to lymphoid organs. *Nat Immunol.* 2006;7:827–834. doi: [10.1038/ni1365](https://doi.org/10.1038/ni1365)
 24. Manni M, Gupta S, Ricker E, Chinenov Y, Park SH, Shi M, Pannellini T, Jessberger R, Ivashkiv LB, Pernis AB. Regulation of age-associated B cells by IRF5 in systemic autoimmunity. *Nat Immunol.* 2018;19:407–419. doi: [10.1038/s41590-018-0056-8](https://doi.org/10.1038/s41590-018-0056-8)
 25. Pearce G, Audzevich T, Jessberger R. SYK regulates B-cell migration by phosphorylation of the F-actin interacting protein SWAP-70. *Blood.* 2011;117:1574–1584. doi: [10.1182/blood-2010-07-295659](https://doi.org/10.1182/blood-2010-07-295659)
 26. Murugan AK, Ihara S, Tokuda E, Uematsu K, Tsuchida N, Fukui Y. SWAP-70 is important for invasive phenotypes of mouse embryo fibroblasts transformed by v-Src. *IUBMB Life.* 2008;60:236–240. doi: [10.1002/iub.33](https://doi.org/10.1002/iub.33)
 27. Ripich T, Chacon-Martinez CA, Fischer L, Pernis A, Kiessling N, Garbe AI, Jessberger R. SWEF proteins distinctly control maintenance and differentiation of hematopoietic stem cells. *PLoS One.* 2016;11:e161060.
 28. Kojonazarov B, Novoyatleva T, Boehm M, Happe C, Sibinska Z, Tian X, Sajjad A, Luitel H, Kriechling P, Posern G, et al. p38 MAPK inhibition improves heart function in pressure-loaded right ventricular hypertrophy. *Am J Respir Cell Mol Biol.* 2017;57:603–614. doi: [10.1165/rcmb.2016-0374OC](https://doi.org/10.1165/rcmb.2016-0374OC)
 29. Meijles DN, Cull JJ, Markou T, Cooper S, Haines Z, Fuller SJ, O'Gara P, Sheppard MN, Harding SE, Sugden PH, et al. Redox regulation of cardiac ASK1 (apoptosis signal-regulating kinase 1) controls p38-MAPK (mitogen-activated protein kinase) and orchestrates cardiac remodeling to hypertension. *Hypertension.* 2020;76:1208–1218. doi: [10.1161/HYPERTENSIONAHA.119.14556](https://doi.org/10.1161/HYPERTENSIONAHA.119.14556)
 30. Deng KQ, Li J, She ZG, Gong J, Cheng WL, Gong FH, Zhu XY, Zhang Y, Wang Z, Li H. Restoration of circulating MFG8 (Milk fat globule-EGF factor 8) attenuates cardiac hypertrophy through inhibition of Akt pathway. *Hypertension.* 2017;70:770–779. doi: [10.1161/HYPERTENSIONAHA.117.09465](https://doi.org/10.1161/HYPERTENSIONAHA.117.09465)
 31. Zhang WW, Jia P, Lu XB, Chen XQ, Weng JH, Jia KT, Yi MS. Capsid protein from red-spotted grouper nervous necrosis virus induces incomplete autophagy by inactivating the HSP90ab1-AKT-MTOR pathway. *Zool Res.* 2022;43:98–110. doi: [10.24272/j.issn.2095-8137.2021.249](https://doi.org/10.24272/j.issn.2095-8137.2021.249)
 32. Bonam SR, Ruff M, Muller S. HSPA8/HSC70 in immune disorders: a molecular rheostat that adjusts chaperone-mediated autophagy substrates. *Cells.* 2019;8:849. doi: [10.3390/cells8080849](https://doi.org/10.3390/cells8080849)
 33. Tanaka Y, Suzuki G, Matsuwaki T, Hosokawa M, Serrano G, Beach TG, Yamanouchi K, Hasegawa M, Nishihara M. Progranulin regulates lysosomal function and biogenesis through acidification of lysosomes. *Hum Mol Genet.* 2017;26:969–988. doi: [10.1093/hmg/ddx011](https://doi.org/10.1093/hmg/ddx011)
 34. Shibuya H, Yamaguchi K, Shirakabe K, Tonegawa A, Gotoh Y, Ueno N, Irie K, Nishida E, Matsumoto K. TAB1: an activator of the TAK1 MAPKKK in TGF-beta signal transduction. *Science.* 1996;272:1179–1182. doi: [10.1126/science.272.5265.1179](https://doi.org/10.1126/science.272.5265.1179)
 35. Garcia-Rivas G, Castillo EC, Gonzalez-Gil AM, Maravillas-Montero JL, Brunck M, Torres-Quintanilla A, Elizondo-Montemayor L, Torre-Amione G. The role of B cells in heart failure and implications for future immunomodulatory treatment strategies. *ESC Heart Fail.* 2020;7:1387–1399. doi: [10.1002/ehf2.12744](https://doi.org/10.1002/ehf2.12744)
 36. Ocana-Morgner C, Gotz A, Wahren C, Jessberger R. SWAP-70 restricts spontaneous maturation of dendritic cells. *J Immunol.* 2013;190:5545–5558. doi: [10.4049/jimmunol.1203095](https://doi.org/10.4049/jimmunol.1203095)
 37. Ihara S, Oka T, Fukui Y. Direct binding of SWAP-70 to non-muscle actin is required for membrane ruffling. *J Cell Sci.* 2006;119:500–507. doi: [10.1242/jcs.02767](https://doi.org/10.1242/jcs.02767)
 38. Chacon-Martinez CA, Kiessling N, Winterhoff M, Faix J, Muller-Reichert T, Jessberger R. The switch-associated protein 70 (SWAP-70) bundles actin filaments and contributes to the regulation of F-Actin dynamics. *J Biol Chem.* 2013;288:28687–28703. doi: [10.1074/jbc.M113.461277](https://doi.org/10.1074/jbc.M113.461277)
 39. Baranov MV, Revelo NH, Dingjan I, Maraspini R, Ter Beest M, Honigsmann A, van den Bogaart G. SWAP70 Organizes the actin cytoskeleton and is essential for phagocytosis. *Cell Rep.* 2016;17:1518–1531. doi: [10.1016/j.celrep.2016.10.021](https://doi.org/10.1016/j.celrep.2016.10.021)
 40. Oberbanscheidt P, Balkow S, Kuhn J, Grabbe S, Bahler M. SWAP-70 associates transiently with macropinosomes. *Eur J Cell Biol.* 2007;86:13–24. doi: [10.1016/j.ejcb.2006.08.005](https://doi.org/10.1016/j.ejcb.2006.08.005)
 41. Biswas PS, Gupta S, Stirzaker RA, Kumar V, Jessberger R, Lu TT, Bhagat G, Pernis AB. Dual regulation of IRF4 function in T and B cells is required for the coordination of T-B cell interactions and the prevention of autoimmunity. *J Exp Med.* 2012;209:581–596. doi: [10.1084/jem.20111195](https://doi.org/10.1084/jem.20111195)
 42. Beel S, Moisse M, Damme M, De Muynck L, Robberecht W, Van Den Bosch L, Saffig P, Van Damme P. Progranulin functions as a cathepsin D chaperone to stimulate axonal outgrowth in vivo. *Hum Mol Genet.* 2017;26:2850–2863. doi: [10.1093/hmg/ddx162](https://doi.org/10.1093/hmg/ddx162)
 43. Zhou X, Sun L, Bracko O, Choi JW, Jia Y, Nana AL, Brady OA, Hernandez J, Nishimura N, Seeley WW, et al. Impaired prosaposin lysosomal trafficking in frontotemporal lobar degeneration due to progranulin mutations. *Nat Commun.* 2017;8:15277. doi: [10.1038/ncomms15277](https://doi.org/10.1038/ncomms15277)
 44. Zhu Y, Ohama T, Kawase R, Chang J, Inui H, Kanno K, Okada T, Masuda D, Koseki M, Nishida M, et al. Progranulin deficiency leads to enhanced age-related cardiac hypertrophy through complement C1q-induced beta-catenin activation. *J Mol Cell Cardiol.* 2020;138:197–211. doi: [10.1016/j.yjmcc.2019.12.009](https://doi.org/10.1016/j.yjmcc.2019.12.009)
 45. Fukui Y, Ihara S. A mutant of SWAP-70, a phosphatidylinositoltrisphosphate binding protein, transforms mouse embryo fibroblasts, which is inhibited by sanguinarine. *PLoS One.* 2010;5:e14180. doi: [10.1371/journal.pone.0014180](https://doi.org/10.1371/journal.pone.0014180)
 46. Lin HB, Naito K, Oh Y, Farber G, Kanaan G, Valaperti A, Dawood F, Zhang L, Li GH, Smyth D, et al. Innate immune Nod1/RIP2 signaling is essential for cardiac hypertrophy but requires mitochondrial antiviral signaling protein for signal transductions and energy balance. *Circulation.* 2020;142:2240–2258. doi: [10.1161/CIRCULATIONAHA.119.041213](https://doi.org/10.1161/CIRCULATIONAHA.119.041213)
 47. Zhang D, Gaussin V, Taffet GE, Belaguli NS, Yamada M, Schwartz RJ, Michael LH, Overbeek PA, Schneider MD. TAK1 is activated in the myocardium after pressure overload and is sufficient to provoke heart failure in transgenic mice. *Nat Med.* 2000;6:556–563. doi: [10.1038/75037](https://doi.org/10.1038/75037)
 48. Ma ZG, Yuan YP, Zhang X, Xu SC, Kong CY, Song P, Li N, Tang QZ. C1q-tumour necrosis factor-related protein-3 exacerbates cardiac hypertrophy in mice. *Cardiovasc Res.* 2019;115:1067–1077. doi: [10.1093/cvr/cvy279](https://doi.org/10.1093/cvr/cvy279)
 49. Li L, Chen Y, Doan J, Murray J, Molkenkin JD, Liu Q. Transforming growth factor beta-activated kinase 1 signaling pathway critically regulates myocardial survival and remodeling. *Circulation.* 2014;130:2162–2172. doi: [10.1161/CIRCULATIONAHA.114.011195](https://doi.org/10.1161/CIRCULATIONAHA.114.011195)

SUPPLEMENTAL MATERIAL

Data S1. Supplemental Methods

Animal models and echocardiography

All animal experiments were approved by the Institutional Animal Care and Use Committee of the Zhongnan Hospital of Wuhan University (ZN2021201). The mice received humane care in accordance with the Guide for the Care and Use of Laboratory Animals published by the National Institutes of Health. In order to reduce the influence of sex and estrogen, male mice were used in this study. Animal sample size used in this study was determined according to the previous studies related to cardiac hypertrophy (8, 10). Mice were in good health before TAC or sham surgery and had access to food and water ad libitum. C57BL/6 male mice (weight: 25.5-27 g, age: 9-11 weeks) were randomly divided into TAC or sham group, anesthetized with pentobarbital sodium (60 mg/kg), and considered adequate anesthesia with no significant toe contractile reflex. When the breathing rule of mice was stable, male mice were placed in supine position and fixed at a 37°C automatic adjusting heating pad. Then, we cut the skin centered on the collarbone and thoracic junction, and separate the muscles and thymus on both sides. Whereafter, we ligated the exposed aortic arch with 7-0 silk thread and 26-gauge needle to form the aortic arch narrow. Sham group mice only performed surgery but not narrowing the aorta. After the operation, the skin was sutured and the mice were placed in a 37°C chamber to wake up. Four weeks after TAC or sham surgery, the mice were anaesthetized with sodium pentobarbital (60 mg/kg) and then euthanized by cervical dislocation. Then, the body

weights were measured, and the heart was quickly removed, placed in 10% KCL solution to stop the heart in a diastolic phase. Then, hearts were dried, weighed, and pictured. Meanwhile, the lung weight (LW) and tibial length (TL) were measured to calculate the ratios of heart weight (HW) /body weight (BW) (mg/g), HW/TL (mg/mm), and LW/BW (mg/g).

Echocardiography was performed to evaluate cardiac functions at the specified time point by using the Small Animal Ultrasound Imaging System (VEVO2100, FUJIFILM VISUALSONICS, Canada) with 30-MHz (MS400) probe. After calmed animals with 2% isoflurane, we used the M-mode echocardiography at short axis view and obtained the corresponding indexes for three consecutive cycles in the papillary muscle, and gained the heart rate, blood velocity, pressure gradient, left ventricular end systolic diameter, left ventricular end diastolic diameter, left ventricular ejection fraction, fraction shortening of each mouse. No mice died in the experiment. Operations and subsequent analyses were performed in a double blinded fashion.

Generation of Genetically Modified Mice

Swap70-KO mice were generated by using the online CRISPR design system (<http://chopchop.cbu.uib.no/>) to predict the guide sequence of target DNA region (sgRNA: TCAGCACCGTGCACAGGTTATGGG). Then, pUC57-sgRNA (Addgene, 51132) was used as the skeleton vector to construct *Swap70*-sgRNA expression vector. The established *Swap70*-sgRNA expression vector and Cas9 expression vector pST1374-Cas9 (Addgene, 44758) was transfected in vitro, and mixed the purified

RNA products from them. Next, the mixture was injected into the single cell fertilized eggs of C57BL/6 mice using a Femtojet 5247 microinjection system, and transplanted into a surrogate female. After about 19-21 days of gestation, F0 generation mice were obtained and taken the toe tissues for genotype identification with following primers: *Swap70*-check F1: 5'-CTCATGGTGAGCAGGTGAAA-3', and *Swap70*-check R1: 5'-CCCTCATCGTCATCCCTAAA-3'.

Neonatal rat ventricular myocytes (NRVMs) and cell culture

Primary NRVMs were isolated from 1 to 2 days old Sprague-Dawley rats. Hearts were extracted from the body and transferred into 60 mm dish containing ~5ml of DMEM. After removing the auricle and large vessels, the hearts were rinsed to remove blood. Transferred the hearts into another dish containing DMEM and cut the hearts into 1 mm³ pieces. Transferred the heart tissue to a 50 mL tube containing 10 mL of 0.125% trypsin-EDTA. Placed the tube on shaker at 120 rpm at 37°C for 7 min. The myocardial tissues were digested for 7-10 times and terminated with DMEM medium containing 20% fetal bovine serum (FBS). Next, cell suspension was filtered through a cell filter to remove large impurities and centrifuged at 1500 rpm to get cell precipitation. Red blood cell lysis buffer was used to remove the erythrocytes and terminated with at least 10 times the volume of DMEM medium. Whereafter, cell precipitates were obtained by centrifugated at 1500 rpm. The mixed precipitation was cultured with DMEM medium containing 10% FBS, 1% penicillin/streptomycin for 1-2 h to allow fibroblasts and endothelial cells to adhere, then the supernatant was

collected and centrifuged at 1500 rpm to get NRVMs. The cells yield and viability were determined. NRVMs were cultured with DMEM/F 12 medium containing 10% FBS, 1% penicillin/streptomycin, and 0.1 mM BrdU (ST1056, Beyotime, China). After 24 h culturing in a complete medium, NRVMs were infected with the corresponding adenoviruses at a 50 multiplicity of infection. Then, the cells were treated with 50 μ M phenylephrine (PE, P6126, Sigma) for indicated hours to induce cardiomyocyte hypertrophy. Cycloheximide (25 μ M), chloroquine (25/50 μ M), MG132 (50 μ M), and 5Z-7-oxozeaenol (100 nM) were used for indicated experiments. Human embryonic kidney (HEK) 293 and 293T cells were cultured in DMEM (C11995, Gibco, Grand Island, NY, USA) containing 10% FBS and 1% penicillin-streptomycin, and identified with no mycoplasma contamination.

Histological staining analysis

For histological assay, mice and human heart tissues were collected and embedded in paraffin. After dewatering and embedding, the heart wax block was sectioned horizontally with a thickness of 5 μ m. Using hematoxylin (G1004, Servicebio) & eosin (BA-4024, Baso) and picosirius red (26357-02, Hedebiotecnology) staining, we got the cardiac myocyte cross-sectional area and collagen fiber content of mice model. And the expression of SWAP70 (A14857, ABclonal, 1:100 dilution) in human heart tissues was determined by immunohistochemical staining through the stain of corresponding index. Digital image analysis system (Image-Pro Plus Version 6.0) was used to statistic images form above pictures.

Immunofluorescence staining

NRVMs were inoculated on slides of 24 well plate at a density of $1.2-1.5 \times 10^5$ cells each well. After infected with corresponding adenoviruses, NRVMs were washed and fixed with 4% formaldehyde at room temperature for 15 min. Then, washed the slides three times with PBS and transparent with 0.5% Triton-X 100 (T8787, Sigma-Aldrich) for 15 min at room temperature, blocked with 8% goat serum for 30-60 min at 37°C. Whereafter, the slides were incubated with indicated primary antibodies over night at 4°C and corresponding secondary antibodies for 1 hours at 37°C. Images were obtained using the inverted fluorescence microscope or confocal laser scanning microscope (TCS SP8, LEICA, Wetzlar, Germany). The antibodies are listed in **Table S1**.

Plasmid Construction and Viral Infection

Plasmids like *Swap70*, *Grn*, *Hsp90ab1*, and *Hspa8* were acquired from the human/rat cDNA by PCR-based cloning and inserted into the vector with the appropriate label. The shuttle plasmid pENTR-U6-CMV-flag-T2A-EGFP (for knockdown virus), pENTR-CMV-flag-T2A-EGFP or pENTR-CMV-flag/HA (for overexpression virus) were used for the construction of gateway plasmids with or without EGFP, and control viruses were constructed with empty plasmids for later experiments. Then, we used ViraPower Adenoviral Expression System (V493-20; Invitrogen; Carlsbad, CA, USA) to turn our target sequences into the adenoviral vectors (pAd/PL-DEST), and

linearized them by PacI (R0547L; NEB; MA, USA). Next, we purified those adenoviral vectors and transfected them into HEK 293 cells with polyethyleneimine (PEI; 24765-1; Polysciences; Warrington, UK) transfection reagent. After intermittent fluid exchange and observation, cells were harvested after 7-9 days to obtain the initial adenovirus. And after 3-4 generations of amplification, the corresponding adenovirus was harvest, liquid nitrogen freezing and thawing, and purified by cesium chloride density gradient centrifugation. Finally, the titer was measured by a 50% tissue culture infective dose method using HEK 293 cells. The primers for plasmid construction and sequencing are listed in **Table S2**.

Western Blot Analysis

Cells and cardiac tissues were obtained, and lysed by RIPA lysis buffer (P0013E; Beyotime Biotechnology; Shanghai, China). After fully cleavage, liquid was centrifugated at 1200 g for 10 min to get the supematant containing proteins. Then, the protein content was quantified using a BCA protein quantification kit according to the manufacturer's instructions (23225; Thermo Fisher Scientific; Waltham, MA, USA). After quantification, proteins were boiled at 95°C for 10-15 min, added into 15 wells concentrated glue, separated by 10% or 12% SDS-PAGE, and transferred to 0.45 µm PVDF membranes (IPVH00010; Millipore; Billerica, MA, USA). Later, PVDF membranes were closure for 1 h with TBST containing 5% skim milk, incubated overnight at 4°C with indicated primary antibodies, and followed with 1 h incubation of corresponding secondary antibodies. Finally, we used the ECL kit (170-

5061; Bio-Rad; Hercules, CA, USA) according to the manufacturer's instructions to detect the protein level, and the ChemiDoc MP Imaging System (Bio-Rad; Hercules, CA, USA) was used to visualize the protein. The antibodies are listed in **Table S1**.

Quantitative real Time PCR (qRT-PCR)

After obtaining the heart tissues and cells, we extracted the total RNA by using the TRIzol reagent and phenol-chloroform method, and dissolved it into DEPC water. Then, 1-2 μg RNA was reverse transcribed into complementary DNA (cDNA) and analyzed by using specific primers in qRT-PCR system (LightCycler 480 Instrument II). GAPDH serves as an internal reference gene, and $2^{-\Delta\Delta\text{CT}}$ method was used to quantitatively determine the gene expression. The primers used are listed in **Table S3**.

Immunoprecipitation Assays

For immunoprecipitation (IP) assays. HEK 293T cells transfected with the indicated plasmids or NRVMs infected with indicated adenovirus were lysed by IP lysis buffer (20 mM Tris-HCl, pH 7.4; 150 mM NaCl; 1 mM EDTA; and 1% NP-40) at 4°C. After centrifugation at 1200 g for 10 min, the samples were purified with 13 μl protein A/G agarose beads (AA104307; Bestchrom, Shanghai, China) for 1 h and incubated with 20 μl protein A/G agarose beads containing 1 μl indicated primary antibodies overnight at 4°C. Then, the beads were successively washed with cold 300 mM or 150 mM IP buffer three times, respectively. After washing, beads were resuspended with 2 \times SDS loading buffer and boiled at 95°C for 15 min. Western blot analysis was

employed to exam the relation between proteins. For IP-mass spectrometry analysis, the immunoprecipitation complex was collected, separated by 10 well separation gel, sliver stained, and sent to Shanghai applied protein technology (APT) Co., Ltd., Shanghai, China. The antibodies are listed in **Table S1**.

RNA-Seq and Analysis

Total RNA was collected from WT or *Swap70*-KO mice with TAC surgery. According to the manufacturer's instructions, cDNA libraries were constructed using an MGIEasy Library Prep Kit. Then, the RNA was improved to a single-ended libraries (50 bp) and sequenced using the MGISEQ-2000 RS. The sequencing fragments were filtered and mapped to the mouse reference genome (mm10/GRCm38) using HISAT2 software. The mapped fragments were first transferred into the BAM format using SAM-tools, and then estimated the Fragments Per Kilobase of exon model per Million mapped fragments (FPKM) of each detected gene using StringTie software. Finally, DESeq2 was chose to quantify the differentially expressed genes (DEGs) based on the criteria below: the log fold change was greater than 2 and the corrected P value is less than 0.05.

Principal component analysis (PCA): PCA is a linear dimension reduction algorithm and a commonly used data pre-processing method. Its goal is to use Variance to measure the variance of data, and to project the highly different high-dimensional data into the low-dimensional space for representation. In most cases, we want to obtain two principal component factors, named principal component 1 and principal

component 2, which are extracted from the directions with the greatest and second greatest difference in data, respectively.

Kyoto encyclopedia of genes and genomes (KEGG) enrichment analysis: KEGG database integrate genomic, chemical, and phylogenetic functional information. Through the Fisher's exact test, all the differential genes were performed by KEGG pathway enrichment analysis, and the corresponding KEGG pathway annotations were downloaded latter. Pathways with p-values less than 0.05 were identified as significantly enriched pathways.

Gene Set Enrichment Analysis (GSEA): According to the KEGG pathway, GSEA was performed to sort genes according to the degree of differential expression, and obtained the total change of these gene set. GSEA was performed on the Java GSEA platform using the "Signal 2 Noise" metric. Gene sets were considered statistically significant with a p value < 0.05 and a false discovery rate (FDR) < 0.25 . Based on the biological events in the process of myocardial hypertrophy (fibrosis, heart function and protein processing) got by GSEA, the genes related to these events were extracted and ranked according to their contribution degree. Then, according to the contribution degree, the top 30 genes were selected, and R-packet heatmap was used to draw the heatmap to show the expression of each gene in the two groups.

Table S1. List of antibodies

Antibody	Cat No.	Manufacturer
SWAP70	A14857	Abclonal
SAPK/JNK	9252	CST
Phospho-SAPK/JNK(Thr183/Tyr185)	4668	CST
Phospho-p38 MAPK (Thr180/Tyr182)	4511	CST
p38 MAPK	8690	CST
Phospho-TAK1 (Thr184/187)	4508S	CST
TAK1	5206	CST
ANP	27426-1-AP	proteintech
BNP	A2179	Abclonal
MYH7	22280-1-AP	proteintech
α -actinin	3134	CST
Lamp1	1D4B	DSHB
Lamp1	9091	CST
GRN	A5773	Abclonal
AKT	A17909	Abclonal
Phospho-AKT	4060	CST
IKK β	A0714	Abclonal
Phospho- IKK α/β	2694	CST
Flag	M185-3LL	MBL
Flag	20543-AP	proteintech
HA	M180-3	MBL
HA	3724S	CST
GAPDH	60004-1-Ig	proteintech
Goat anti-mouse IgG (H+L)	115-035-003	Jackson
Goat anti-rabbit IgG (H+L)	111-035-003	Jackson

568 Goat anti-rabbit IgG (H+L)	A11036	invitrogen
488 Goat anti-mouse IgG (H+L)	A11029	invitrogen
568 Goat anti-mouse IgG (H+L)	A11031	invitrogen
488 Goat anti-rabbit IgG (H+L)	A11034	invitrogen

Table S2. Primer for Plasmid construction and sequencing

Human	
Phage-3xFlag- SWAP70	F TCGGGTTTAAACGGATCCATGGGGAGCTTGAAGGAGGAGC R GGGCCCTCTAGACTCGAGTCACTCCGTGGTCTTTTTCTCTTTCC
PcDNA5-HA- GRN	F TCGGGTTTAAACGGATCCATGTGGACCCTGGTGAGCT R GGGCCCTCTAGACTCGAGCAGCAGCTGTCTCAAGGCT
PcDNA5-HA- HSP90AB1	F TCGGGTTTAAACGGATCCATGCCTGAGGAAGTGCACCATG R GGGCCCTCTAGACTCGAGATCGACTTCTTCCATGCGAGAC
PcDNA5-HA- HSPA8	F TCGGGTTTAAACGGATCCATGTCCAAGGGACCTGCAG R GGGCCCTCTAGACTCGAGTCAACCTCTTCAATGGTGGGC

Rat	
Ad-GFP-Flag- <i>Grn</i>	F GGCTAGCGATATCGGATCCGCCACCATGCCTCCCAGGGAGCG R CGTCCTTGTAATCACTAGTCAGTAGCGGTCTTGGGGCTG
Ad-Flag- <i>Grn</i>	F GGCTAGCGATATCGGATCCGCCACCATGCCTCCCAGGGAGCG R TGCCACCCGTAGATCTTCACTTGTCATCGTCGTCCTTGTAATCCAG TAGCGGTCTTGGG
Ad-GFP-Flag- <i>Swap70</i>	F GGCTAGCGATATCGGATCCGCCACCATGGGGGGCTTGAAAGACG R CGTCCTTGTAATCACTAGTGTCTGTGGTCTTCTTCTTTCCAG
Ad-HA- <i>Swap70</i>	F GGCTAGCGATATCGGATCCATGGGGGGCTTGAAAGACGAAC R CCCGTAGATCTTCAAGCGTAATCTGGAACATCGTATGGGTAGTCT GTGGTCTTCTTCTC
Ad-GFP-Flag- <i>Swap70 aa</i>	F GGCTAGCGATATCGGATCCGCCACCATGCGTCAGACAGTGTCTAT GG

193-585 R CGTCCTTGTAATCACTAGTGTCTGTGGTCTTCTTCTC

Ad-GFP-Flag- F GGCTAGCGATATCGGATCCGCCACCATGGCGGCGCAGAGGAGG

Tab1 R CGTCCTTGTAATCACTAGTAGGTGCCGTCATCACACTCTGC

Ad-GFP-sh- F CCGGGGACAAAGTGGCCCATCATGACTCGAGTCATGATGGGC

Swap70 CACTTTGTCCTTTTTG

R AATTCAAAAAGGACAAAGTGGCCCATCATGACTCGAGTCATGA

TGGGCCACTTTGTCC

Ad-GFP-sh- F CCGGGGTGCTGAACCATTGCCTTATCTCGAGATAAGGCAATGG

Tak1 #1 TTCAGCACCTTTTTG

R AATTCAAAAAGGTGCTGAACCATTGCCTTATCTCGAGATAAGG

CAATGGTTCAGCACC

Ad-GFP-sh- F CCGGGCTGAACCATTGCCTTATTACCTCGAGGTAATAAGGCAA

Tak1 #2 TGGTTCAGCTTTTTG

R AATTCAAAAAGCTGAACCATTGCCTTATTACCTCGAGGTAATA

AGGCAATGGTTCAGC

Ad-GFP-sh- F CCGGGCAGCCCAAAGCTCTCATTCACTCGAGTGAATGAGAGCT

Tak1 #3 TTGGGCTGCTTTTTG

R AATTCAAAAAGCAGCCCAAAGCTCTCATTCACTCGAGTGAATG

AGAGCTTTGGGCTGC

Ad-GFP-sh- F CCGGGCCCAAAGCTCTCATTATAGCTCGAGCTATGAATGAGA

Tak1 #4 GCTTTGGGCTTTTTG

R AATTCAAAAAGCCCAAAGCTCTCATTATAGCTCGAGCTATGA

ATGAGAGCTTTGGGC

plasmid sequencing (phage-flag)

CMV-F CGCAAATGGGCGGTAGGCGTG

MPGK-R TGGAATGTGTGCGAGGCCAG

plasmid sequencing (PcDNA5-flag/HA)

CMV-F CGCAAATGGGCGGTAGGCGTG

BGH CAGGGTCAAGGAAGGCAC

plasmid sequencing (pENTR-U6-CMV-flag-T2A-EGFP)

U6 ATGGACTATCATATGCTTACCGTA

plasmid sequencing (pENTR-CMV-flag-T2A-EGFP)

CMV-F CGCAAATGGGCGGTAGGCGTG

pEGFP-N-3 CGTCGCCGTCCAGCTCGACCAG

plasmid sequencing (pENTR-CMV-flag/HA)

CMV-F CGCAAATGGGCGGTAGGCGTG

hGH-

Poly(A)-R GGTCACAGGGATGCCACC

plasmid sequencing (pAd/PL-DEST)

pAd-For GACTTTGACCGTTTACGTGGAGAC

pAd-Rev CCTTAAGCCACGCCACACATTC

Table S3. Primers for PCR

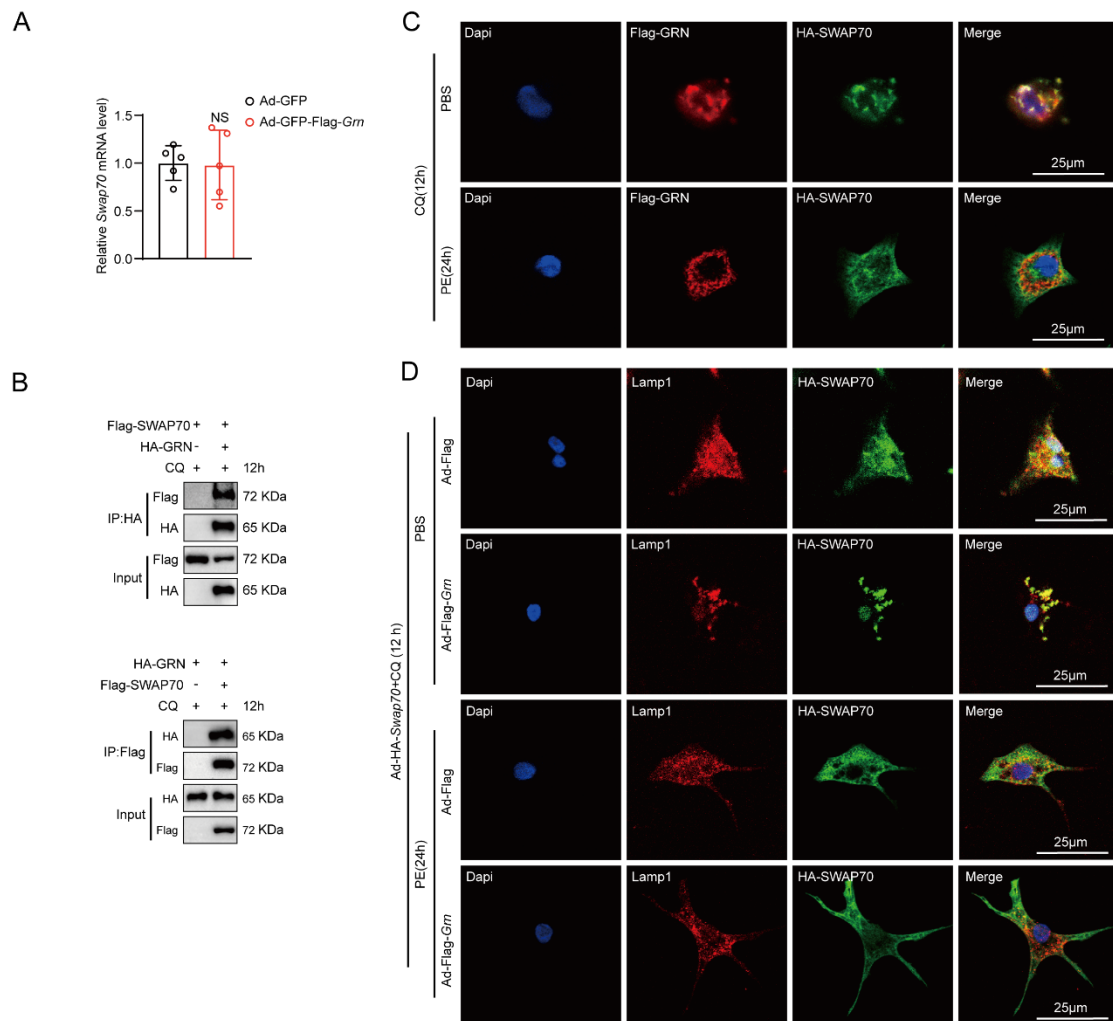
Human		
ANP	F	CCCATGTACAATGCCGTGTC
	R	GGCAGATCGATCAGAGGAGT
BNP	F	TGGAAACGTCCGGGTTACAGGA
	R	TCCGGTCCATCTTCCTCCCAA
MYH7	F	GGGCAAAGGCAAGGCCAAGAAA
	R	ATGGGTGGAGCGCAAGTTGGTCA
SWAP70	F	TTTACAGCGAGTACGGGAGC
	R	TCTTCCTCCAACAACCTGGC
GAPDH	F	CATCACCATCTTCCAGGAGCGAGA
	R	TGCAGGAGGCATTGCTGATGATCT
Mice		
<i>Anp</i>	F	TCGGAGCCTACGAAGATCCA
	R	TTCGGTACCGGAAGCTGTTG
<i>Bnp</i>	F	GAAGGACCAAGGCCTCACAA
	R	TTCAGTGCGTTACAGCCCAA
<i>Myh7</i>	F	CAACCTGTCCAAGTTCCGCA
	R	TACTCCTCATTGAGGCCCTTG
<i>Collagen Ia1</i>	F	TGCTAACGTGGTTCGTGACCGT
	R	ACATCTTGAGGTCGCGGCATGT
<i>Collagen</i>	F	ACGTAAGCACTGGTGGACAG
<i>IIIa1</i>	R	CCGGCTGGAAAGAAGTCTGA
<i>Ctgf</i>	F	TGACCCCTGCGACCCACA
	R	TACACCGACCCACCGAAGACACAG
<i>Timp1</i>	F	GAGACCACCTTATACCAGCGTT

	R	TACGCCAGGGAACCAAGAAG
	F	ACTCCACTCACGGCAAATTC
<i>Gapdh</i>	R	TCTCCATGGTGGTGAAGACA
	F	TAGTCCTTCCTACCCCAATTTCC
<i>Il6</i>	R	TTGGTCCTTAGCCACTCCTTC
	F	CCGTGGACCTTCCAGGATGA
<i>Il1β</i>	R	GGGAACGTCACACACCAGCA
	F	CATCTTCTCAAATTCGAGTGACAA
<i>Tnfa</i>	R	TGGGAGTAGACAAGGTACAACCC

Rat

	F	AAAGCAAACCTGAGGGCTCTGCTCG
<i>Anp</i>	R	TTCGGTACCGGAAGCTGTTGCA
	F	TGCCCCAGATGATTCTGCTC
<i>Bnp</i>	R	TGTAGGGCCTTGGTCCTTTG
	F	AGTTCGGGCGAGTCAAAGATG
<i>Myh7</i>	R	CAGGTTGTCTTGTTCGCCT
	F	AGAGTGTGCGGAAGATCAGAC
<i>Swap70</i>	R	CATGTCTTCCAGCTCCCGAA
	F	AGCAGAAACGACAAGGCACT
<i>Tak1</i>	R	TTTGGCATTTCAGAACACGCC
	F	ACTCTACCCACGGCAAGTTC
<i>Gapdh</i>	R	TGGGTTTCCCGTTGATGACC

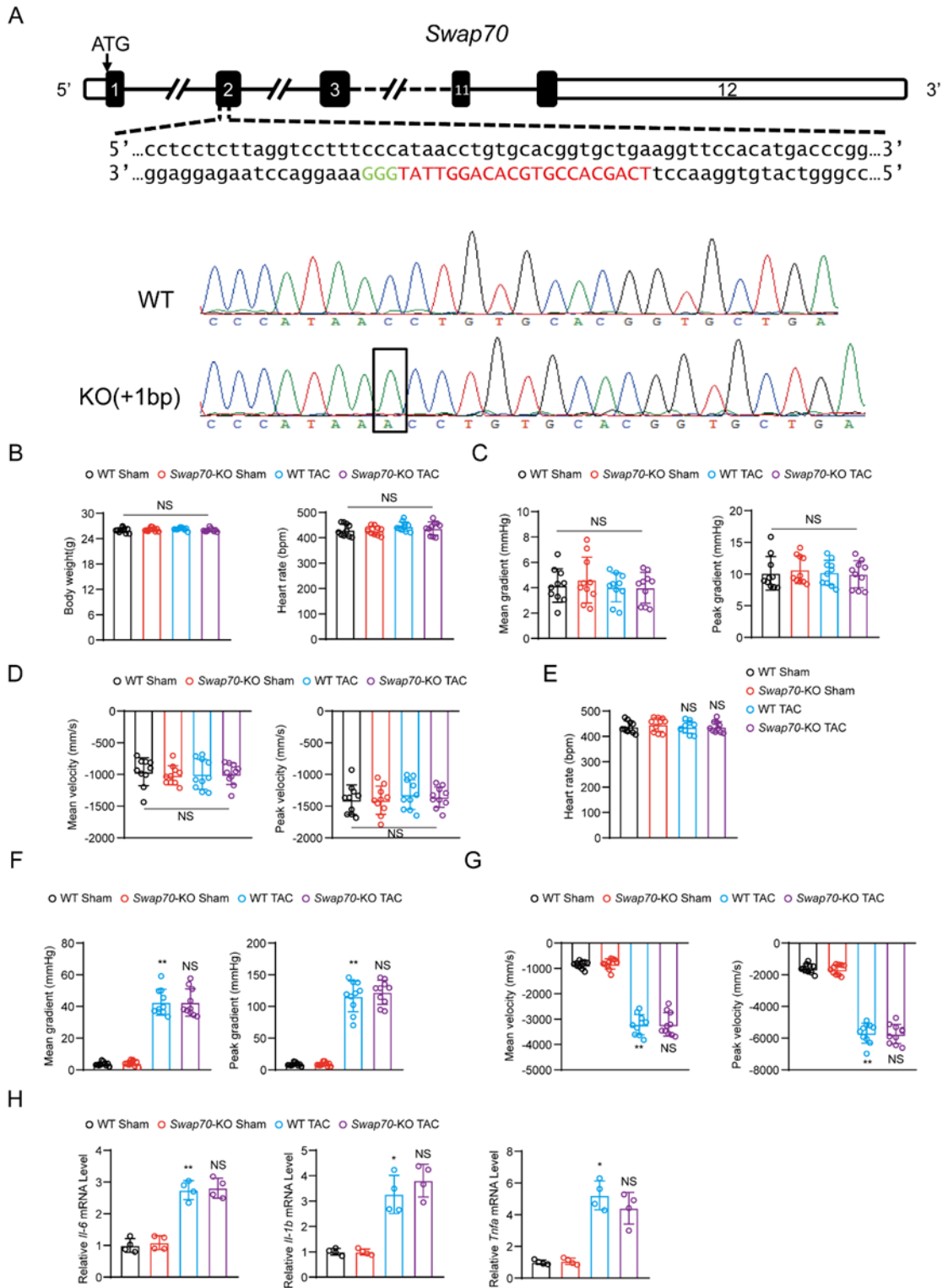
Figure S1. Supplement to Figure 2. Hypertrophic increase in SWAP70 is connected with the inhibition of lysosomal degradation regulated by granulin precursor.



(A) Relative mRNA expression of switch-associated protein 70 (*Swap70*) in neonatal rat ventricular myocytes (NRVMs) infected with indicated adenovirus (n=5 independent experiments) (NS: P=0.92). **(B)** Co-immunoprecipitation (CO-IP) assays displayed the interaction between SWAP70 and granulin precursor (GRN) in human embryonic kidney 293T cells in the presence of cycloheximide (CQ, 25µM). **(C)** Representative immunofluorescence images of the colocalization of SWAP70 and GRN in NRVMs added with CQ (25 µM), Ad-HA-*Swap70* and Ad-Flag-*Grn* adenoviruses in the presence or absence of phenylephrine (PE, 50 µM). **(D)** Representative

immunofluorescence images of the colocalization of SWAP70 and lysosome marker lysosomal associated membrane protein 1 (LAMP1) in NRVMs accompanied with indicated adenoviruses and treatments. Scar bar, 25 μ m. Data are shown as mean \pm SD. Student t test was used. NS, no significance.

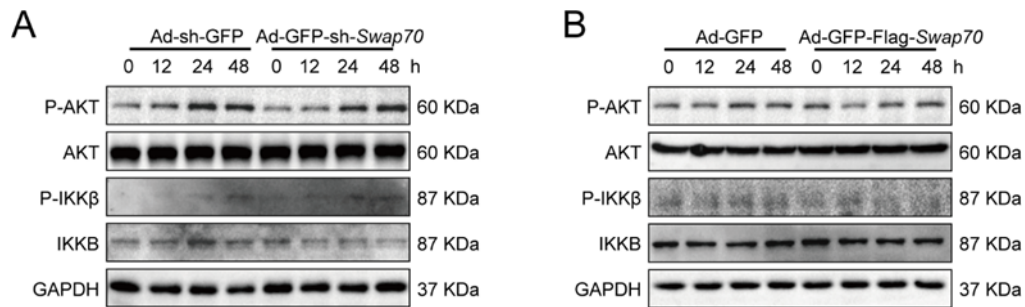
Figure S2. Mouse construction model, ultrasonic data, and inflammation level of each group.



(A) Schematic diagram of switch-associated protein 70 knock out (*Swap70*-KO) mouse model construction. We transformed the 221 to 222 bases of *Swap70* from AC into AAC

to silence the expression of *Swap70*. **(B-D)** Body weight (g), heart rate (bpm), mean gradient (mmHg), peak gradient (mmHg), mean velocity (mm/s), and peak velocity (mm/s) in wide type (WT) and *Swap70*-KO mice before surgery (n=10). **(E-G)** Heart rate (bpm), mean gradient (mmHg), peak gradient (mmHg), mean velocity (mm/s), and peak velocity (mm/s) in WT and *Swap70*-KO mice at 4 weeks after sham or transverse aortic constriction (TAC) surgery (n=10). **(H)** Relative mRNA levels of inflammatory (Insulin 6 [*Il6*], *Il1b*, tumor necrosis factor α [*Tnfa*]) related genes in mice heart tissues from indicated groups (n=4). one-way ANOVA with Bonferroni's post hoc analysis (**B-E**, mRNA levels of *Il6* in **H**) or with Tamhane T2 post hoc test (**F-H**) were used. Kruskal-Wallis nonparametric statistical test (peak gradient in **C**) was used for nonnormal distribution data. *, $P < 0.05$; **, $P < 0.01$ for WT TAC group versus WT sham group. NS (no significance) for indicated group versus control group or *Swap70*-KO TAC group versus WT TAC group (Right in **E, G, H**).

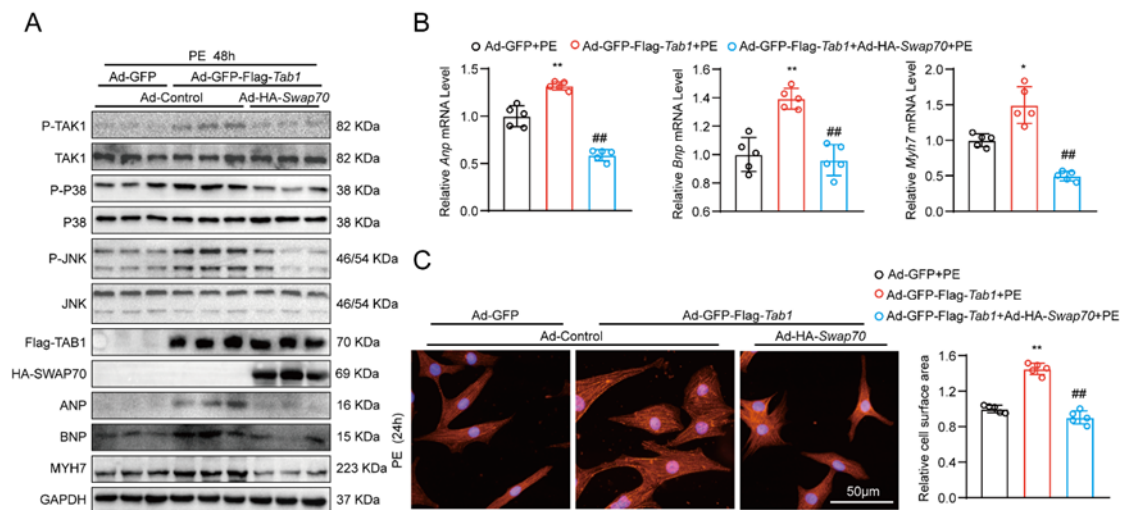
Figure S3. SWAP70 did not influence the activation of AKT and IKK β under hypertrophic stimuli.



(A) Immunoblotting analysis of phosphorylation and total AKT, I-kappa-B-kinase beta (IKK β) proteins in neonatal rat ventricular myocytes (NRVMs) from indicated groups.

(B) Immunoblotting analysis of phosphorylation and total AKT, IKK β proteins in NRVMs infected with indicated adenovirus and stimulated with phenylephrine (PE, 50 μ M) for a time gradient.

Figure S4. SWAP70 regulates cardiac hypertrophy by suppressing the interaction between TAK1 binding protein 1 (TAB1) and TAK1.



(A) Immunoblotting analysis of phosphorylation and total transforming growth factor β -activated kinase 1 (TAK1), P38, JNK1/2 proteins in neonatal rat ventricular myocytes (NRVMs) infected with indicated adenoviruses and stimulated with phenylephrine (PE, 50 μ M) for 48 h, hypertrophic marker proteins (natriuretic peptide A (ANP), natriuretic peptide B (BNP), β -myosin-heavy-chain (MYH7)) were used to assess the severity of the hypertrophy (n=5 independent experiments). (B) Relative mRNA levels of hypertrophic marker genes (*Anp*, *Bnp*, and *Myh7*) in NRVMs from indicated groups (n=5 independent experiments). (C) Representative immunofluorescence images (left) of NRVMs infected with indicated adenovirus in the presence of PE (50 μ M) for 24 h, and stained with α -actinin. Scar bar, 50 μ m. Quantitative results (right) of the cell surface area from indicated groups (n=5 independent experiments). Data are shown as mean \pm SD. One-way ANOVA with Bonferroni's post hoc analysis (mRNA levels of *Bnp* in B, C) or with Tamhane T2 post hoc test (B) were used. *, P < 0.05; **, P < 0.01 for *Tab1* group versus GFP group. ##, P < 0.01 for *Swap70 Tab1* group versus *Tab1*

group.